JOSÉE SEIGNEUR

INTERACTIONS NEURONES-GLIE :
L'ACh et les glies lors de la transition sommeil vers l'éveil *in vivo*

Mémoire présenté
à la Faculté des études supérieures de l'Université Laval
dans le cadre du programme de maîtrise en neurobiologie
pour l'obtention du grade de maître ès sciences (M.Sc.)

FACULTÉ DE MÉDECINE
UNIVERSITÉ LAVAL
QUÉBEC

OCTOBRE 2004

Résumé

Cette étude résume l'historique de la découverte des glies, détaille leur morphologie et leur physiologie. Elle vise principalement à la compréhension des interactions complexes entre les neurones, les glies et l'apport en sang au cortex pendant la transition du sommeil à ondes lentes vers l'éveil *in vivo* chez des animaux anesthésiés et naturellement endormis. Nous effectuons des enregistrements intracellulaires simultanés de neurones et de glies corticaux, conjointement avec les mesures du débit sanguin cérébral, de la concentration extracellulaire de K^+ et les potentiels de champs locaux sous anesthésie pendant l'activation corticale évoquée avec une stimulation électrique des noyaux cholinergiques ou lors de l'éveil naturel de l'animal. Nous suggérons que le résultat du comportement de la glie dépende de l'influence glutamatergique/GABAergique des neurones voisins, sur la modulation des voies de communications intergliales, et/ou sur le trafic ionique au travers des vaisseaux sanguins.

Abstract

This study summarizes the history of the glial discovery, details their morphology and their physiology and aims at understanding complex interactions between cortical neurons, glia and blood supply during the transition from slow wave sleep to wakefulness *in vivo* in both anesthetized and naturally sleeping animals. We performed simultaneous intracellular recordings of cortical neurons and glia, together with measurements of cerebral blood flow, extracellular K^+ concentrations and local field potentials under anesthesia, during elicited cortical activation with electric stimulation of cholinergic nuclei or under naturally wakefulness of the animal. We suggest that the outcome of the glial behavior depends on the glutamatergic/GABAergic influence of neighboring neurons, on the modulation of the interglial communication pathways, and/or on the ionic traffic across blood vessels.

Avant-Propos

L'introduction de ce mémoire débute par un historique sur les mécanismes cérébraux impliquant la transition du sommeil à ondes lentes vers l'éveil, puis il se poursuit sur les données récentes sur les glies. Le mémoire contient un chapitre présentant un article soumis pour la publication et une conclusion générale résumant les principaux sujets abordés dans l'article.

L'article présenté dans ce mémoire est le résultat des expériences que j'ai réalisées dans le laboratoire du Dr Florin Amzica. Je tiens sincèrement à remercier le Dr Amzica de m'y avoir accueilli à bras ouverts et de m'avoir offert son soutien, sa gentillesse et sa grande disponibilité tout au long de ma maîtrise. Je tiens à remercier également le Dr Mircea Steriade pour m'avoir donné une plus grande perspective des neurosciences, de même que Pierre Giguère, Denis Drolet et tous mes collègues étudiants pour leur collaboration professionnelle et morale.

Je dédie cette thèse à mes parents Ghyslaine et Marc pour leur amour, leur présence et leur soutien, de même qu'à mon Amour Christian pour ses mots d'encouragements et pour avoir su répondre à mes caprices tout au long de mes études.

Table des matières

1. Introduction....1
1.1 Historique, morphologie et fonctions des glies....2
1.2 Propriétés électrophysiologiques et canaux ioniques de la membrane gliale....3
1.2.1 Courants potassiques....4
1.2.2 Canaux calciques....4
1.2.3 Transport du Na^+ et du Cl^-....5
1.3 Contrôle de la concentration de K^+ extracellulaire par la glie....6
1.4 Oscillations lentes du sommeil (1 Hz) et états d'activation de l'EEG....7
1.4.1 Les oscillations lentes du sommeil....8
1.4.1.1 Les neurones pendant les oscillations lentes....8
1.4.1.2 Les glies pendant les oscillations lentes....9
1.4.2 La transition du sommeil vers l'éveil....9
1.4.2.1 Les systèmes ascendants cholinergiques....10
1.4.2.1.1 L'organisation du PPT....10
1.4.2.1.2 L'organisation du NB (BF)....12
1.5 Effet de l'ACh sur la glie....13
2. Cholinergic action on cortical glial cells in vivo....14
2.1 Résumé....15
2.2 Abstract....16
2.3 Introduction....17
2.4 Materials and methods....19
2.4.1 Animal preparation....19
2.4.2 Electrodes and recording....20
2.4.2.1 Intracellular recordings and neuroanatomy....20
2.5 Results....24
2.5.1 Database....24
2.5.2 Activation patterns in glia....24
2.5.3 Glia-neuronal relationship during EEG activation....26
2.5.4 Iontophoretic application of ACh on glia....27

2.5.5 Input resistance and membrane capacitance of glia during EEG activation. 27
2.5.6 Muscarinic and glutamatergic components 28
2.5.7 Blood flow behavior during activation 30
2.6 Discussion 30
2.6.1 Consequences of the glial/vascular behavior during cholinergic activation. 34
3. Conclusion 57
Bibliographie 59

Liste des abréviations

$[Ca^{+2}]_{ext}$	Concentration de calcium extracellulaire	
$[K^{+}]_{ext}$	Concentration de potassium extracellulaire	
HCO_3	Ion carbonate	
4-AP	4-aminopyridine	
ACh	Acétylcholine	Acetylcholine
AMPA	acide α-amino-3-hydroxy-5-methyl-4-isoxalepropionique	α-amino-3-hydroxy-5-methyl-4-isoxalepropionique acid
Ba	Barium	
BF	Prosencéphale basal	Basal forebrain
bhB	Bande horizontale de Broca	
bvB	Bande verticale de Broca	
C	Capacitance	Capacitance
CBF	Débit sanguine cérébral	Cerebral blood flow
CNQX	6-Cyano-7-nitroquinoxaline-2,3-dione	
Cs	Césium	
DC	Courant discontinu	Discontinuous current
EEG	Électroencéphalogramme	Electroencephalogram
E_K	Potentiel d'équilibre	
EMG	Électromyogramme	Electromyogram
EOG	Électroocculogramme	Electroocculogram
GABA	Acide gamma-aminobutyrique	Gamma-aminobutyric acid
GFAP	protéine acide fibrillaire gliale	Glial fribrillary acidic protein
IP_3	Inositol 1,4,5-triphosphate	
JCs	Jonctions communiquantes	Gap junctions
LC	Locus cœruleus	
LDT	Noyau latérodorsal tegmental	Laterodorsal tegmental nucleus
mAChR	Récepteurs muscariniques	Muscarinic recepteur

nAChR	Récepteurs nicotiniques	Nicotinic recepteur
NB	Noyau basal (de Meynert)	Nucleus basalis
NMDA	Acide *N*-methyl-*D*-aspartique	*N*-methyl-*D*-aspartic acid
PBS	Tampon phosphate saline	Phosphate buffer saline
PPSE	Potentiel post-synaptique excitateur	
PPSI	Potentiel post-synaptique inhibiteur	
PPT	Noyau pédonculopontine tegmental	Pedonculopontin tegmental nucleus
R	Résistance	Resistance
SI	Substantia Innominata	
SWS	Sommeil à ondes lentes	Slow wave sleep
TBS	Tampon Tris saline	Tris buffer saline
TEA	Tetraethylammonium	
TTX	Tetrodotoxine	Tetrodotoxin
V_m	Potentiel membranaire	Membrane potential
W	Éveil	Wakefulness
τ	Constante de temps	Time constant

Liste des figures

Figure 1: Hyperpolarizing responses in astrocytes after PPT activation. 36

Figure 2: Glial hyperpolarization in a chronically implanted cat during natural transition between slow wave sleep (SWS) and wakefulness (W). 38

Figure 3: Comparison between electrically elicited and spontaneously occurring activation in a pair of simultaneously impaled neuron and glia in a cat under ketamine & xylazine anesthesia. 40

Figure 4: Double intracellular recording (neuron-glia pair) in the suprasylvian gyrus displaying glial depolarization during BF-elicited activation.....42

Figure 5: Iontophoretic application of ACh induced glial hyperpolarization. 44

Figure 6: Iontophoretic application of ACh on neuron. 46

Figure 7: Membrane resistance and capacitance during PPT activation in a simultaneously impaled neuron-glia pair. 48

Figure 8: Muscarinic antagonist scopolamine abolishes V_m hyperpolarization and membrane resistance increase in glia. 50

Figure 9: Cholinergic effect after blockage of kainate/quiscalate glutamatergic receptors with CNQX. 52

Figure 10: Cerebral blood flow (CBF) in association with glial hyperpolarizing responses to cerebral activation. 54

Figure 11: CBF in association with glial depolarizing responses to cerebral activation. 56

1. Introduction

L'intérêt de ce mémoire a été de déterminer l'action des récepteurs cholinergiques sur les membranes des cellules gliales corticales pendant un état de transition entre le sommeil à ondes lentes et l'éveil. Malgré le fait que la présence de récepteurs cholinergiques a été précédemment observée sur la membrane des cellules gliales, la plupart des études ont été faites sur des cellules en culture et/ou *in vitro*, et leur réponse à ce neurotransmetteur a été peu étudiées *in vivo* lors de changements physiologiques.

Les découvertes récentes positionnent les cellules gliales comme un élément interagissant avec les neurones en modulant leur activité synaptique (Barres and Barde, 2000, Araque and al, 1999, Perea and Araque, 2002, Perea and Araque, 2003). Car, tout comme les neurones, les membranes des cellules gliales ont démonté des récepteurs pour les mêmes neurotransmetteurs que les neurones (Eng and al, 1971, Hosli and Hosli, 1993, Porter and McCarthy, 1997). De plus, les cellules gliales possèdent la capacité de libérer des neurotransmetteurs tels l'acide gamma–aminobutyrique (GABA) (MacVicar and al, 1989) et le glutamate (Araque and al, 2000). Tout laisse croire que les cellules gliales ont la propriété de moduler l'information des neurones présents dans son environnement ; ce qui devient d'autant plus d'intérêt lors des changements d'états de vigilances et lors d'états pathologiques tels l'épilepsie.

Les sections suivantes révisent sommairement l'historique de la découverte des glies dans le système nerveux central ainsi que les propriétés morphologiques et électrophysiologiques des glies et leurs fonctions. L'accent a été mis plus particulièrement sur leur participation à la récupération du K^+ extracellulaire ($[K^+]_{ext.}$). De plus, elles mettent en lumière les connaissances obtenues sur le sommeil à ondes lentes, sa transition vers l'éveil et la participation des neurones et des glies lors de ce changement.

1.1 Historique, morphologie et fonctions des glies

La découverte d'éléments différents des neurones a été faite pour la première fois dans le système nerveux central par Dutrochet en 1824 (Privat and al, 1995) qui les décrivit comme des *corpuscules globuleux*, mais c'est Virchow en 1846 qui les nomma *Nevenkitt*. Ce mot a été traduit plus tard par neuroglie. À cette époque, la neuroglie était considérée comme une substance connective dans laquelle les neurones sont incrustés.

La distinction entre les astrocytes fibreux et protoplasmiques a été faite par Andriezen en 1893 (Privat and al, 1995). Il utilisa la méthode de Golgi pour distinguer les glies fibreuses situées principalement dans la matière blanche et les glies protoplasmiques situées dans la matière grise. Par des techniques d'imprégnation au carbonate d'argent, Rio Hortega en 1919-1920 et en 1932 fit la distinction entre les oligodendrocytes et la microglie.

Tout comme les neurones, les cellules gliales ont pour origine le tube neural durant le développement embryonnaire (Kandel and al, 1991). Numériquement, les cellules gliales sont dix fois plus nombreuses que les neurones. La taille de leur corps cellulaire varie de 15-30 μm selon leur fonction et leur emplacement dans le système nerveux central (SNC). Morphologiquement, les astrocytes protoplasmiques possèdent de courts prolongements radiaux, tandis que les astrocytes fibreux ont une apparence étoilée avec leurs longs prolongements peu ramifiés. Les oligodendrocytes avec leurs fins prolongements cytoplasmiques parallèles de 15 à 30 μm de longueur s'enroulent autour des axones des neurones et forment la myéline. La microglie est présente dans la substance grise et elle possède de nombreux prolongements ramifiés dans toutes les directions. L'arrivée de la microscopie électronique a permis de mieux distinguer les microstructures des glies. Ainsi, les astrocytes ont démontrées des gliofilaments qualifiés par (Eng and al, 1971) et (Bignami and al, 1972) comme étant la protéine acide fibrillaire gliale (GFAP). Quant à la microglie, elle se distingue des autres cellules gliales, car elle est la seule cellule qui exprime le récepteur pour le complément CR3 qui lient les lectines (Graeber and al, 1988).

Les fonctions attribuées à chacun des types de cellules gliales ont aussi pris racine à partir d'observations faites au tournant du XXième siècle. Golgi observa en 1885 (Privat and al, 1995) des contacts fréquents entre les prolongements des astrocytes et les vaisseaux

sanguins. Il suggéra que ce type de cellules apportait les nutriments aux neurones. À son tour, His en 1889 suggéra que les glies chez l'embryon servent de guide à la migration des neurones en développement. De plus, Lugaro en 1907 suggéra que les astrocytes adultes servaient de tampon pour maintenir le milieu interstitiel compatible à la fonction des neurones. Enfin, Ramón y Cajal en 1909 proposa sans faire de distinction entre les fonctions des oligodendrocytes et de la microglie que les prolongements des glies servaient d'isolement pour les neurones et qu'elles avaient la possibilité de proliférer pour remplir l'espace extracellulaire en présence d'une lésion. Il est maintenant établi que les oligodendrocytes sont impliqués dans la myélinisation et l'isolation des axones pour la conduction de l'influx nerveux, alors que la microglie peut effectuer la phagocytose des débris cellulaires. Elle joue donc un rôle de défense contre les corps étrangers (Streit, 1995).

L'étude des changements de potentiel membranaire (V_m) des cellules gliales *in vivo* a été rendue possible grâce à l'invention par J.F. Toennies d'un amplificateur capable d'enregistrer avec des électrodes à haute impédance qui a permis par la suite les enregistrements intracellulaires (Brock and al, 1952). La découverte que les glies ont également une membrane polarisée par enregistrement intracellulaires a été faite par Villegas et al (1963)et Kuffler à partir de 1964.

1.2 Propriétés électrophysiologiques et canaux ioniques de la membrane gliale

La glie doit son potentiel de repos de –90 mV, tout près du potentiel d'équilibre (E_K) à sa grande concentration de canaux potassiques sur sa surface membranaire. La membrane gliale présente une résistance membranaire plus basse que les neurones (~10-20 MΩ *in vivo*) et des constantes de temps plus rapides (~200 μs) (Amzica and Neckelmann, 1999, Trachtenberg and Pollen, 1970). Les études électrophysiologiques faites sur les glies ont démontré que leur membrane possède des canaux ioniques similaires aux neurones.

1.2.1 Courants potassiques

Quatre types de courants potassiques ont été principalement observés sur la glie (Duffy and al, 1995, Tse and al, 1992). Le courant entrant I_{IR} (inward rectifier) est le courant le plus important pour l'établissement du V_m glial, car il est le seul courant avec une haute probabilité d'ouverture aux alentours du potentiel de repos. Il a la propriété d'augmenter avec l'hyperpolarisation, il est dépendant de la concentration extracellulaire de K^+ et il peut être bloqué par le Cs ou le Ba extracellulaire. Il est aussi dépendant de la concentration extracellulaire de Na^+ (Ransom and al, 1996). Les glies possèdent également des courants potassiques sortants. Le courant I_k (I_{DR}; delayed rectifier) a été trouvé en culture où la plupart des cellules gliales ont un V_m autour de –40 mV (Duffy and al, 1995). Il est inactif au V_m de repos et il est activé par la dépolarisation (~ -40 mV). Il peut être bloqué par le Cs intracellulaire, le TEA, le 4-AP ou le Ba extracellulaire. Le courant I_A est semblable à celui observé chez les neurones. Il est transitoire, complètement inactivé au V_m de repos, il s'active à un seuil autour de ~-40 mV et s'inactive rapidement avec la dépolarisation. Il peut être bloqué par le Cs ou par le 4-AP. Les glies montrent aussi des courants calcium et voltage dépendants $I_{K(Ca)}$. Les canaux impliquant ses courants sont de deux sous-types de conductances différentes: I_{SK} (25 pS) et I_{BK} (230 pS) qui peuvent être bloqués par le TEA extracellulaire. Le courant I_{SK} est un courant sortant activé par la dépolarisation et bloqué par un influx de Ca^{2+} voltage-dépendant (Quandt and MacVicar, 1986). Par la dépolarisation, l'influx de Ca^{2+} augmente la perméabilité membranaire au K^+ et pourrait donc augmenter la capacité des cellules gliales à capturer le K^+ extracellulaire. Le courant I_{BK} est aussi sensible au tamponnage du Ca^{2+} intracellulaire (Barres and al, 1990).

1.2.2 Canaux calciques

Les astrocytes montrent la présence de canaux calciques voltage-dépendants et des canaux calciques associés à un ligand. La présence de canaux calciques voltage-dépendants a été démontrée en enregistrant un courant de type L sensible à la nifedipine (MacVicar and Tse, 1988) en culture. Toutefois, leur expression ne semble pas être constitutive (Corvalan and al, 1990) et elle est dépendante de la présence des neurones ou du taux d'AMPc intracellulaire. De plus, des courants de type L et T ont pu être observés chez les astrocytes

isolés à partir du nerf optique. Les études faites par les techniques d'enregistrements de patch clamp ou d'intracellulaire ne révèlent pas la présence de courants voltage-dépendants. (Duffy and MacVicar, 1994, Carmignoto and al, 1998) Toutefois, il ne peut pas être exclu que les astrocytes puissent exprimer ce type de canaux. Il est possible qu'ils soient exprimés en faible densité ou que leur inactivation soit trop rapide pour être détectée.

Les canaux calciques associés aux ligands sont de deux types : ils peuvent être liés aux récepteurs acide α-amino-3-hydroxy-5-methyl-4-isoxalepropioniqie (AMPA), un sous-type des récepteurs au glutamate, et aux purinorécepteurs. L'activation des récepteurs AMPA dans les cultures d'astrocytes bloquent les courants K^+ par une augmentation du Na^+ interne (Robert and Magistretti, 1997). Aucune évidence n'a été faite quant à la présence de récepteurs calciques ligand-dépendants à l'acide *N*-methyl-*D*-aspartique (NMDA) (Teichberg, 1991). Les purinorécepteurs détectés chez les astrocytes sont non spécifiques pour les cations.

1.2.3 Transport du Na^+ et du Cl^-

Le transport du Na^+ et du Cl^- est couplé à plusieurs fonctions homéostatiques des astrocytes. Les astrocytes présentent un courant I_{Na} qui peut être bloqué par du TTX et d'autres courants sodiques qui sont couplés à des courants potassiques sortants (I_{DR},I_A) (Robert and Magistretti, 1997) ou au transport de neurotransmetteurs (Pellerin and Magistretti, 1994). Par exemple, le rôle essentiel de capturer l'excès de glutamate dans la fente synaptique est achevé par un co-transporteur glutamate/Na^+. Conséquemment l'entrée de Na^+ génère une augmentation de $[Na^+]_i$ qui permet l'activation de l'ATPase Na^+/K^+. Similairement, le co-transporteur $Na^+/K^+/2Cl^-$ joue un rôle dans la récupération du K^+ pendant l'activité neuronale (Tas and al, 1986). Les astrocytes présentent également un canal Cl^- voltage-dépendant qui s'active à un V_m dépolarisé. Contrairement aux neurones, le $GABA_A$ aurait un effet dépolarisant sur la membrane des astrocytes en ouvrant les canaux Cl^-. Ce phénomène est rendu possible à cause du potentiel de Nernst de l'ion Cl^- est autour de –40 mV (MacVicar and al, 1989). La membrane gliale possède aussi des co-transporteurs Na^+/HCO_3 (O'Connor and al, 1994) et des co-transporteurs $K^+/Cl^-/HCO_3$ responsables du gonflement des cellules (Bekar and Walz, 1999). Les cellules gliales

possèdent des canaux Cl^- volumes-sensitifs ($I_{Cl(swell)}$) qui s'ouvrent par une voie autocrine impliquant des récepteurs purinergiques. Ces canaux sont activés par la libération d'ATP par les astrocytes lors du gonflement cellulaire (Darby and al, 2003). La liberation d'ATP contribue à la propagation de la vague calcique et peut influencer l'excitabilité neuronale (Guthrie and al, 1999). Le gonflement cellulaire est contrebalancé par une perte de volume impliquant un efflux de métabolites et une activation des courants $I_{Cl(swell)}$ et K^+.

1.3 Contrôle de la concentration de K^+ extracellulaire par la glie

Le contrôle de la concentration de K^+extracellulaire est une des fonctions les plus connues de la glie (Newman, 1995). La concentration normale extracellulaire est autour de 3 mM et une petite augmentation de moins de 1 mM a été mesurée durant les activités normales (Singer and Lux, 1975, Amzica and Steriade, 2000). Toutefois, pendant les crises épileptiques, de plus grandes variations de la concentration en potassium ont été mesurées et la $[K^+]_{ext.}$ peut atteindre 9-10 mM (Moody and al, 1974). La concentration plafonne à 12 mM suggérant que des mécanismes de régulation efficaces soient présents dans le système nerveux. Les variations de la $[K^+]_{ext.}$ influencent l'activité des neurones en modifiant le potentiel d'équilibre du K^+; la force conductrice pour les différents courants voltage- et ligand-dépendants (Newman, 1995). Donc, les variations de $[K^+]_{ext.}$ constituent un signal d'interaction entre la glie et les neurones.

Les cellules gliales sont pourvues de mécanismes passifs et actifs de capture du K^+. La capture passive de K^+ est produite par des influx de K^+ accompagnés par des influx de Cl^- contrôlés par les forces de Donnan et/ou par le transport couplé via les co-transporteurs $Na^+/K^+/2Cl^-$ ou K^+/Cl^-. Toutefois, la perméabilité au Cl^- est sous régulée par la capture passive de K^+. Les canaux chlore sont à leur tour contrôlés par les récepteurs $GABA_A$ présents sur la membrane gliale (Bormann and Kettenmann, 1988, MacVicar and al, 1989, Rosier and al, 1993). La capture active de potassium a lieu à la fois dans les neurones et les glies par l'intermédiaire des pompes Na^+/K^+ ATPase. De plus, les cellules gliales possèdent des pompes plus nombreuses et plus efficaces que les neurones (Walz and Hertz, 1982).

Les pompes des glies saturent à des niveaux plus élevés que celles des neurones (Franck and al, 1983).

La redistribution spatiale du K^+ peut se produire à travers l'espace extracellulaire selon le gradient de diffusion ou à l'intérieur des réseaux de cellules gliales par une dispersion intracellulaire de l'ion (Nicholson, 1995, Orkand and al, 1966, Orkand, 1986). Également nommé tamponnage spatial, la dispersion intracellulaire consiste à transporter ces ions de régions de hautes concentrations vers d'autres à des concentrations plus faibles en utilisant les passages par les jonctions communiquantes (JCs) (Newman, 1986). Le tamponnage spatial s'applique aux deux situations suivantes: (i) lors d'une augmentation locale de $[K^+]_{ext.}$, le tamponnage permet une entrée ponctuelle du K^+ dans le milieu intracellulaire et occasionne un transport net de K^+ à travers de JCs dans le syncytium, (ii) lors d'une augmentation étendue de la $[K^+]_{ext.}$ pendant d'une grande activité neuronale, il permet une récupération massive du K^+ et cela occasionne une dépolarisation globale de la glie. Des estimations des constantes d'espace ont indiqué que le tamponnage peut s'étendre sur quelques centaines de micromètres (Gardner-Medwin and Nicholson, 1983, Gardner-Medwin, 1983).

1.4 Oscillations lentes du sommeil (1 Hz) et états d'activation de l'EEG

L'animal anesthésié est un modèle couramment utilisé pour étudier le sommeil à ondes lentes. En plus de démontrer un électroencéphalogramme (EEG) similaire à celui des animaux préparés de façon chronique, l'animal en préparation aiguë paralysé et anesthésié sous ketamine-xylazine ou sous uréthane maintient dans un état de vigilance constant en plus de favoriser l'enregistrement stable de cellules. De cette manière, il est plus aisé d'obtenir des résultats reproductibles. L'animal sous anesthésie demeure un modèle de choix pour étudier le sommeil. Toutefois, les données obtenues ne peuvent pas être extrapolées au sommeil naturel. Pour cette raison, il est aussi préférable de déterminer ce qu'il se produit chez l'animal en préparation chronique. Toutefois, il demeure difficile d'obtenir des enregistrements stables de cellules chez un animal en mouvement.

Le chat est un sujet préférentiellement choisi dans le but d'étudier le sommeil à cause de la similarité des états de vigilances avec l'humain (éveil, sommeil à ondes lentes, sommeil paradoxal) et par sa prédisposition au sommeil pendant la journée. Les différents stades de vigilances chez le chat sont décrits en détails chez le chat par (Ursin, 1968).

1.4.1 Les oscillations lentes du sommeil

Le sommeil à ondes lentes est dominé par une oscillation lente de l'EEG inférieure à 1 Hz (principalement 0.5-0.9 Hz). Cette oscillation de moins d'1 Hz est bien caractérisée dans les variations du potentiel membranaire pendant le sommeil (Amzica and Steriade, 1998b). L'oscillation lente a été observée durant le sommeil naturel chez le chat (Steriade and al, 2001, Steriade and al, 1996, Amzica and Steriade, 1998a) et chez l'humain (Amzica and Steriade, 1997, Achermann and Borbely, 1997, Simon and al, 2000), ainsi que sous anesthésie avec l'uréthane, la kétamine-xylazine ou l'oxyde d'azote (Contreras and Steriade, 1995, Steriade and al, 1994a, Steriade and al, 1993c, Steriade and al, 1993b). Elle regroupe d'autres rythmes de sommeil tels les fuseaux et les ondes delta (Amzica and Steriade, 1995, Contreras and Steriade, 1995, Amzica and Steriade, 1998b, Steriade and Amzica, 1998). L'oscillation lente est générée à l'intérieur des réseaux corticaux puisqu'elle survit dans les préparations athalamiques et *cerveau isolé* (Steriade and al, 1993c). Elle est également absente du thalamus chez le chat ayant subi l'ablation du cortex (Timofeev and Steriade, 1996). L'origine corticale de l'oscillation lente est de plus supportée par sa distribution laminaire avec un bassin principal dans les couches corticales II-III (Amzica and Steriade, 1998a). Le cortex endormi apparaît comme un oscillateur maître, en imposant son rythme lent au thalamus et en modulant les activités ayant comme origine le thalamus (Steriade and al, 1994b).

1.4.1.1 Les neurones pendant les oscillations lentes

Durant l'oscillation lente, le potentiel membranaire des neurones corticaux alterne entre des phases de dépolarisations et d'hyperpolarisations (Steriade and al, 1993b). La phase dépolarisée correspond à une excitation générale des neurones corticaux et cela occasionne des potentiels post-synaptiques excitateurs (PPSEs), des potentiels d'actions et des

potentiels post-synaptiques inhibiteurs (PPSIs) (Amzica and Steriade, 1995). La présence synchronisée de potentiels d'action dans virtuellement tous les neurones corticaux durant cette phase d'oscillation lente (Amzica and Steriade, 1995) est probablement accompagnée par une libération de K^+ dans l'espace extracellulaire. Au niveau de l'EEG, la dépolarisation est associée avec une déflection négative profonde (Contreras and Steriade, 1995). En ce qui concerne les hyperpolarisations longues, elles ont été associées avec une absence de décharge de tous les neurones corticaux induisant de cette façon une disfacilitation généralisée dans le réseau cortical (Contreras and al, 1996). Récemment, il a été démontré que cette disfacilitation est induite par deux mécanismes : (1) une baisse progressive du Ca^{+2} extracellulaire $[Ca^{+2}]_{ext}$ ayant lieu durant la phase de dépolarisation de l'oscillation lente réduit l'efficacité synaptique (Massimini and Amzica, 2001), et (2) l'excitabilité neuronale est modulée par la régulation gliale du K^+ extracellulaire (Amzica and Massimini, 2002).

1.4.1.2 Les glies pendant les oscillations lentes

Les cellules gliales oscillent avec les neurones durant les ondes lentes du sommeil (Amzica and Neckelmann, 1999, Amzica and Massimini, 2002). De plus, comme il a été montré avec des doubles enregistrements, le V_m glial a une dynamique distincte du V_m du neurone. La phase dépolarisée dans les neurones est associée avec une dépolarisation progressive et décalée de la glie. La phase neuronale d'hyperpolarisation est précédée par le début d'une repolarisation lente de la glie. De plus, une variation similaire de $[K^+]_{ext.}$ et du V_m de la glie confirment que les cellules gliales jouent principalement un rôle de capture du K^+ extracellulaire (Amzica and al, 2002). Donc, la phase dépolarisante de l'oscillation lente est associée avec une augmentation graduelle de la $[K^+]_{ext.}$.

1.4.2 La transition du sommeil vers l'éveil

La transition du sommeil à ondes lentes vers l'éveil est sous le contrôle, entre autres, de systèmes modulateurs cholinergiques. Les neurones du mésencéphale de la formation réticulée augmentent leur taux de décharge environ 15 s avant la fin des épisodes de

sommeil, ce qui provoque l'éveil et ils gardent leur taux de décharge plus élevé durant l'éveil que pendant le sommeil à ondes lentes (Steriade and al, 1982).

1.4.2.1 Les systèmes ascendants cholinergiques

Les neurones relâchant l'acétylcholine (ACh) sont localisés principalement dans deux agrégats cellulaires : le premier à la jonction mésopontine [le noyau pédonculopontine tegmental (PPT) (Jones and Cuello, 1989) et le noyau latérodorsal tegmental (LTD)] et le second dans le noyau basal (NB) de Meynert du prosencéphale basal (BF).

1.4.2.1.1 L'organisation du PPT

Il est connu depuis longtemps que la stimulation électrique de la formation réticulée du mésencéphale produit une activation de l'EEG (Moruzzi and Magoun, 1949) et une libération d'ACh au cortex (Celesia and Jasper, 1966). Chez l'humain, le noyau pédonculopontin tegmental a été décrit par comme un agrégat de grands neurones qui s'étendent de la limite caudale du noyau rouge au noyau péribrachial, en étroite association avec le pédoncule cérébelleux supérieur. Il peut être subdivisé en deux sous-noyaux selon la densité cellulaire : la *pars compacta* et la *pars dissipata*. Le PPT est un agrégat hétérogène aussi bien du point de vue de la cytochimie que de la morphologie. Actuellement, il est accepté que le PPT contient des neurones cholinergiques et non cholinergiques (Spann and Grofova, 1992). Les neurotransmetteurs utilisés par les neurones non cholinergiques du PPT ne sont pas tous définis. Des neurones glutamatergiques ont été détectés chez le rat (Grofova and Zhou, 1998) et le primate (Lavoie and Parent, 1994). Les deux types de neurones contiennent une grande variété de peptides dont entre autre la substance P. Il n'est toutefois pas exclu que quelques neurones du PPT puissent utiliser le GABA comme neurotransmetteur (Vincent and al, 1983, Charara and al, 1996).

Le noyau pédonculopontin tegmental possède une grande variété de projections grâce à ses nombreuses collatérales. Le PPT reçoit de nombreuses afférences provenant des neurones GABAergiques des ganglions de la base, des neurones sérotoninergiques du noyau de raphé (Steininger and al, 1997), des projections catécolaminergiques du *locus cœruleus* (LC) et les projections cholinergiques du PPT contralatéral et du LDT ipsilatéral (Semba and

Fibiger, 1992). Étant donné que la majorité des influx que reçoivent les neurones du PPT sont inhibiteurs, il est possible que seul la déinhibition des neurones du PPT permette son activation (Winn and al, 1997).

Le PPT possède aussi de nombreuses efférences divisées en voies descendantes et ascendantes. Les projections ascendantes du PPT sont situées dans la portion centrale du mésencéphale tegmental et elles se divisent en deux : une portion ventromédiale et une autre dorsolatérale, et elles se dirigent vers les structures du mésencéphale et du diencéphale et vers le cortex préfrontal médial. Chez le chat, aucune voie directe vers le cortex n'a été observé. La plupart des projections ascendantes passent vers l'hémisphère contralatéral par les commissures (Sugimoto and Hattori, 1984). Les afférences et les efférences sont pour la plupart réciproques (Takakusaki and al, 1996, Scarnati and al, 1987, Goldsmith and van der, 1988, Semba and al, 1990) et elles arrivent aux deux parties du PPT, *pars compacta* et *pars dissipata*, bien que préférentiellement elles se dirigent vers les grands neurones non cholinergiques de la *pars dissipata.*

Les fonctions du PPT sont variées. Il participe à l'activité motrice, au comportement émotionnel et au contrôle du cycle sommeil-éveil.

Dans le contexte de la transition du sommeil à ondes lentes vers l'éveil, les projections majoritairement cholinergiques du PPT et du LDT vers les noyaux intralaminaires de la ligne médiane du thalamus sont considérés comme faisant partie du système réticulaire activateur ascendant qui dépolarisent les neurones glutamatergiques thalamocorticaux et produisent une désynchronisation de l'EEG (Jones, 1991). Les projections ascendantes du PPT atteignent massivement les noyaux intralaminaires de la ligne médiane du thalamus, bien que le PPT projette également vers le noyau réticulaire et les noyaux de relais majoritairement moteurs et sensoriels du thalamus. Cela diffère du LDT qui projette vers les noyaux thalamiques limbiques ou d'association (Scarnati and al, 1987, Sugimoto and Hattori, 1984, Hallanger and Wainer, 1988, Sofroniew and al, 1985).

La libération d'ACh au niveau du thalamus induit l'éveil et le sommeil paradoxal, provoquant une dépolarisation des neurones thalamocorticaux qui passent d'un mode de décharge tonique à phasique, La décharge phasique des neurones thalamocorticaux

interrompe la synchronisation entre le thalamus et le cortex. La décharge tonique du thalamus associée avec le sommeil lent cesse lors de la libération d'acétylcholine et les neurones toniques retournent dans un état hyperpolarisé permettant aux cellules du noyau réticulé du thalamus de décharger de façon tonique et de produire la synchronisation de l'EEG. La suppression des oscillations lentes du sommeil se produit par déinhibition des circuits locaux inhibiteurs du tronc cérébral (Datta and Siwek, 1997).

1.4.2.1.2 L'organisation du NB (BF)

Le prosencéphale basal contient des neurones cholinergiques et GABAergiques qui sont entremêlés avec différents types d'interneurones contenant les peptides somatostatin et neuropeptide Y. Tous ont la possibilité de projeter directement au cortex (Zaborszky, 1999 1143 /id). Tandis que les neurones ascendants du PPT-LDT sont relayés par les neurones glutamatergiques thalamocorticales, le NB est pourvu de projections directes vers le cortex (Steriade and McCarley, 1990, Wainer and Mesulam, 1990). Le terme noyau basal de Meynert est aussi employé pour les neurones cholinergiques dans la bande horizontale (bhB) et verticale de Broca (bvB), la substancia innominata (SI) et les aires péripallidales qui projettent vers le cortex. Le BF reçoit des afférences du cortex, des ganglions de la base du LC et du noyau pédonculopontin tegmental. En effet, le PPT offre un lien avec la sous population de cellules cholinergiques dans le NB et les aires qui l'entourent (Jones and Cuello, 1989, Semba, 1991). De plus, l'aire cholinergique du PPT contrôle orthodromiquement un cinquième des neurones du BF qui projettent vers le cortex (Jones and Cuello, 1989, Semba and al, 1988). L'augmentation de l'ACh suite à une stimulation du PPT suggère fortement que les neurones cholinergiques du BF sont activés par la stimulation du PPT (Consolo and al, 1990). Il a été trouvé que l'activation provoquée par la stimulation du BF ne peut être bloquée par microdialyse d'antagonistes muscariniques ou nicotiniques. Elle a été substantiellement substantiellement réduite par l'application d'un antagoniste glutamatergique, l'acide kynuréique (Rasmusson, 1994 1148 /id). De plus, l'ACh inhibe les neurones cholinergiques *in vitro* (Khateb, 1997 1149 /id) suggérant que l'influx excitateur du BF provenant du PPT est de nature glutamatergique. À cet effet, il a été aussi démontré que des neurones cholinergiques projettent vers les neurones GABAergiques du BF (Vazquez and Baghdoyan, 2003).

Plusieurs données supportent l'hypothèse que les neurones du BF relaient l'influence activatrice glutamatergique provenant de la formation réticulée du tronc cérébral au cortex. D'abord, une corrélation entre l'EEG cortical et les profiles de décharges des neurones du BF a été démontré. Puis, une stimulation du noyau mésencéphalique supérieur permet augmentation de la libération d'ACh dans le cortex cérébral (Celesia and Jasper, 1966, Szerb, 1967).

1.5 Effet de l'ACh sur la glie

L'application d'ACh sur des astrocytes *in vitro* a donné dans la majorité des cas une hyperpolarisation marquée (Hosli and Hosli, 1993, Hosli and al, 1988). L'effet de l'ACh sur la glie corticale est réalisé dans les astrocytes protoplasmiques et fibreux principalement par l'intermédiaire de récepteurs muscariniques (Van Der Zee and al, 1993, Van Der Zee and al, 1989). Des analyses biochimiques ont démontré la présence de récepteurs muscariniques en présence de carbachol ou d'oxotremorine (Meeker and Harden, 1982, Tanner and al, 1986). De plus, l'activation des mAChs stimulent le métabolisme phosphoinositide et la mobilisation du calcium dans l'hippocampe (Araque and al, 2002). En utilisant des antagonistes radioactifs (Hosli and Hosli, 1988), les astrocytes ont montré des sites de liaisons partout sur les corps cellulaires et les processus. L'activité neuronale peut réguler le pourcentage de mAChRs sur les astrocytes (Beldhuis and al, 1992). Les récepteurs nicotiniques ont été aussi trouvés en autoradiographie sur des cultures, mais ils ont une incidence plus faible que les récepteurs muscariniques (Hosli and Hosli, 1988). Les études in vivo (Smiley and Lieberman, 1980, Villegas, 1975) et en culture (Hosli and al, 1988) démontrent que l'ACh serait le seul neurotransmetteur qui hyperpolarise la glie. Le glutamate et le GABA ont un effet dépolarisant.

L'objectif de ce mémoire était d'étudier l'effet de l'ACh sur les cellules gliales corticales *in vivo* dans un contexte *in situ* où les cellules gliales reçoivent l'ACh des structures sous-corticales, c'est-à-dire lors de la transition du sommeil à ondes lentes vers l'éveil. Par le fait même, l'étude a mis l'accent sur les interactions entre les neurones et les glies et sur l'implication du système cérébrovasculaire lors de cette transition.

Chapitre 2|
Cholinergic action on cortical glial cells in vivo

Josée Seigneur and Florin Amzica*

Article en révision, Cerebral Cortex (août 2004)

2.1 Résumé

L'objectif de cette étude est la compréhension des interactions complexes entre les neurones, les glies et l'apport en sang au cortex pendant la transition du sommeil à ondes lentes vers l'éveil. En dépit des données essentielles provenant des préparations *in vitro* et en culture, les mécanismes de base des interactions de la glie avec son environnement cellulaire et ionique demeurent non investigué *in vivo*. Ici, nous effectuons des enregistrements intracellulaires simultanés de neurones et de glies corticaux, conjointement avec les mesures du débit sanguin cérébral, de la concentration extracellulaire de K^+ et les potentiels de champs locaux chez des animaux anesthésiés et naturellement endormis. Sous anesthésie, l'activation corticale est évoquée avec une stimulation électrique des noyaux cholinergiques (noyau pédoculopontin tegmental dans le tronc cérébral et/ou le noyau basal du prosencéphale basal). L'application iontophorétique d'acétylcholine sur les cellules enregistrées a été également utilisée. Dans la grande majorité des cas (>80%), les cellules gliales ont été hyperpolarisées durant l'activation électrique ou spontanée. Ce résultat a été également obtenu dans tous les cas où l'iontophorèse a été utilisé ou quand les récepteurs glutamatergiques kainates/quiscalates ont été bloqués avec du CNQX. L'hyperpolarisation gliale est associée avec l'état dépolarisé du neurone, l'augmentation du CBF, une concentration faible de K^+ extracellulaire, une augmentation de la résistance membranaire, une diminution de la capacitance membranaire et des potentiels de champs DC persistants négatifs. Dans plusieurs cas d'activation corticale (<20%), les cellules gliales démontrent des potentiels dépolarisés soutenus, en parallèle avec une dépolarisation neuronale, une diminution du CBF et des potentiels de champs DC plus négatifs. Nous suggérons que le résultat du comportement de la glie dépend de l'influence glutamatergique/GABAergique des neurones voisins, sur la modulation des voies de communications intergliales, et/ou sur le trafic ionique au travers des vaisseaux sanguins.

2.2 Abstract

This study aims at understanding complex interactions between cortical neurons, glia and blood supply developing during the transition from slow wave sleep to wakefulness. In spite of essential advances from *in vitro* and culture preparations, the basic mechanisms of glial interactions with their cellular and ionic environment remained uninvestigated *in vivo*. Here we approach this issue by performing simultaneous intracellular recordings of cortical neurons and glia, together with measurements of cerebral blood flow (CBF), extracellular K^+ concentrations and local field potentials in both anesthetized (ketamine-xylazine) and naturally sleeping cats. Under anesthesia, cortical activation was elicited with electric stimulation of cholinergic nuclei (pedunculopontine tegmental in the brainstem and/or *nucleus basalis* of the basal forebrain). Iontophoretic application of acetylcholine on the recorded cells was also used. In the vast majority of cases (>80%), glial cells were hyperpolarized during electric stimulation of spontaneous activation. This result was also obtained in all cases where iontophoresis was used or when glutamatergic kainate/quisqualate receptors were blocked with CNQX. The glial hyperpolarization was associated with steady neuronal depolarization, increased CBF, low extracellular K^+ concentration, increased membrane resistance, decreased membrane capacitance, and persistent positive DC field potentials. In some cases of cortical activation (<20%), glial cells displayed sustained depolarizing potentials, in parallel with neuronal depolarization, decreased CBF and more negative DC field potentials. We suggest that the outcome of the glial behavior depends on the glutamatergic/GABAergic influence of neighboring neurons, on the modulation of the interglial communication pathways, and/or on the ionic traffic across blood vessels.

2.3 Introduction

By activating the EEG after stimulating the reticular formation of the brainstem, Moruzzi and Magoun (1949) have demonstrated that this structure is critically involved in the modulation of vigilance. Previous studies (reviewed in Wainer and Mesulam, 1990, Steriade and McCarley, 1990) suggest that cholinergic modulatory systems play an essential role during the transition from slow wave sleep (SWS) to wakefulness (W). During SWS and under anesthesia, the electroencephalogram (EEG) is characterized by large amplitude slow waves. These oscillations coincide with alternating periods of depolarization and hyperpolarization of both neurons (Steriade and al, 1993b) and glia (Amzica and Neckelmann, 1999), in parallel with increases and decreases in the extracellular K^+ concentration ($[K^+]_o$) (Amzica and al, 2002). Upon awakening, the slow EEG and neuronal activities are abolished and neurons display fast oscillations around a depolarized membrane potential (V_m) (Steriade and al, 1993a). Previous studies have emphasized the role of glial cells in regulating $[K^+]_o$ (Orkand and al, 1966, Somjen, 1979, Newman, 1995). However, no information is available concerning the behavior of glial cells, $[K^+]_o$ and its regulation during the transition from SWS to W.

This study becomes even more necessary as the exclusive focus on neuronal discharges in understanding conscious phenomena and principles of information processing is not sufficient. Recent reports brought into attention reciprocal neurotransmitter-based exchanges between neurons and glia (Bezzi and Volterra, 2001). This adds to the already known functions of glial cells in regulating extracellular environment, removal of neurotransmitters, as well as development and regeneration. It has been known for some time that glial cells possess receptors for acetylcholine (ACh) (Van Der Zee and al, 1993). In addition, networks of gap junctions between glia enable the rapid propagation of molecules and ions between cells (see Ransom, 1995).

The effect of ACh on cortical neurons has been studied extensively. ACh depolarizes neurons and increases their membrane resistance (Krnjevic and al, 1971, Krnjevic and Reinhardt, 1979). Glial cells were mostly studied *in vitro* and in culture. It was shown that addition of ACh on astrocytes from explant cultures of rat brainstem and spinal cord

elicited membrane hyperpolarization (Hosli and Hosli, 1993, Hosli and al, 1988). In hippocampal slices, glial cells responded to cholinergic stimulation with an intracellular Ca^{2+} elevation mobilized from the internal stores (Araque and al, 2002). As intraglial Ca^{2+} changes may further cause neurotransmitters release (Parpura and al, 1994, Pasti and al, 1997, Bezzi and al, 1998, Araque and al, 2000), it is essential to disclose the behavior of cortical glial cells during behavioral activation.

Although studies performed in slices or cultures have been essential in disclosing glial functions, they cannot, however, recreate the vast network of an intact brain in which glia and neurons interact spontaneously during various vigilance states. To overcome these limitations, our experiments were performed *in vivo*. The activation of the cortex was achieved by electric stimulation of cholinergic nuclei located either in the basal forebrain (BF) or in the brainstem [pedunculopontine tegmental (PPT) nucleus], but also by spontaneous transitions between SWS and W in chronically implanted animals. We aimed at a farther-reaching view by investigating the behavior of glia, blood supply and extracellular space composition during the activated states and in relation with the already known pattern of sleep.

2.4 Materials and methods

2.4.1 Animal preparation

Experiments were performed on both acute and chronic animals. Acute experiments were carried out on 32 adult cats of both sexes, deeply anesthetized with ketamine & xylazine (10-15 mg/kg and 2-3 mg/kg, respectively, i.m.). The depth of anesthesia was continuously monitored by the electroencephalogram (EEG), heart rate and end-tidal CO_2 concentration. Additional doses of anesthetic were given at the slightest tendency toward an activated EEG pattern or accelerated pulse (>110 beats/min). Body temperature was maintained between 37–39°C with a heating pad. Surgical procedures consisted of: cephalic vein canulation for systemic liquid delivery, lidocaine infiltration of all pressure points or incision lines, muscle paralysis with gallamine triethiodide and tracheal cannulation. Cats were artificially ventilated throughout all experiments. Craniotomy exposed the cerebral cortex (suprasylvian gyrus) for insertion of both intracellular and extracellular glass micropipettes. In this preparation, the stability of intracellular recordings was enhanced by cisternal drainage, hip suspension, pneumothorax, and filling of the hole in the calvarium with a 4% agar solution. Glucose (5% solution, 10 ml i.v.) was given every 3–4 h during experiments.

Chronically implanted cats (n = 2) were used to validate the data from anesthetized preparations. Surgical procedures are detailed elsewhere (Steriade and Amzica, 1996). Briefly, the implantation of electrodes for cardinal signs distinguishing natural wake and sleep states (EEG, electromyogram-EMG, and electrooculogram-EOG) was performed under ketamine (15 mg/kg, i.m.) followed by barbiturate anesthesia (25 mg/kg, i.p.). Atropine sulphate (0.05 mg/kg, i.m.) was injected to prevent secretions. A craniotomy with incision of the *dura mater* was equally performed and covered with agar and a plastic cap. Buprenorphine (0.03 mg/kg, i.m.) was given every 12 hours, for 24 hrs, to prevent pain after surgery. An antibiotic (bicillin) was injected i.m. during three days post-operatively. Intracellular and EEG recordings began seven days after surgery. During sessions, the plastic cap above the craniotomy was removed, intracellular pipettes were lowered into the

cortex and the agar pressure foot was renewed. Animals were not deprived of sleep. The method used to keep the head rigid without pain or pressure during the recording sessions was similar to that previously described (Glenn and Steriade, 1982). During recording, the animal could move its limbs and often made postural adjustments.

At the end of the experiments, the animals received a lethal i.v. dose of sodium pentobarbital (50 mg/kg). All experimental procedures were performed according to NIH guiding principles and were also approved by the committee for animal care of Laval University.

2.4.2 Electrodes and recording

2.4.2.1 Intracellular recordings and neuroanatomy

Intracellular recordings from neurons and glia in the cerebral cortex (suprasylvian areas 5 and 7) were obtained with glass micropipettes (tip diameter <0.5 μm) filled with potassium acetate (3 M, *in situ* resistance 35-50 MΩ). In the case of neuronal impalements, only stable recordings with resting membrane potentials (V_m) more negative than -60 mV, overshooting action potentials and input resistances >20 MΩ were accepted for analysis. Intraglial recordings were kept only if displaying a stable V_m more negative than -70 mV without current compensation during the whole recording. No action potentials were fired at impalement, exit or by imposing intracellular depolarizing currents that would bring the V_m close -55 mV. Both upon impalement of (not shown) and leaving (Fig. 1*B*) the glia, a brisk voltage shift, with no action potential discharge, was recorded.

The membrane resistance and capacitance were tested in both neurons and glia during the activation of the EEG by means of intracellularly delivered hyperpolarizing current pulses (50-80 ms duration, 0.5-1 nA intensity). The resistance (R) was calculated as the ratio between the voltage deflection (average of at least 10 ms during the plateau response) and the injected current eliciting that voltage response. The membrane capacitance (C) was obtained from the time constant (τ) of the active response to the current pulses ($\tau = RC$). The time constant was estimated with a double exponential fit (for details see (Amzica and

Neckelmann, 1999) and were in agreement with previous reports (Trachtenberg and Pollen, 1970).

On some occasions, in order to visualize the impaled cells, intraglial recordings were performed with pipettes containing 2% biocytin in the 3 M potassium acetate solution (*in situ* resistance 60-100 MΩ). The cell was filled with biocytin by injecting positive current pulses (200ms, 50% duty cycle) of 0.5-1 nA during at least 10 minutes. At the end of these experiments, animals were perfused with phosphate buffer saline (PBS) followed by a fixative containing 4% paraformaldehyde and 1% glutaraldehyde in PBS (0.1 M, pH 7.4). Brains were cryoprotected with 30% sucrose in paraformaldehyde 4%. Then, 50 µm coronal sections were cut with a Vibratome and processed for fluorescent microscopy. The brain slices were washed in PB 0.1 M and in tris-buffer saline (TBS) 0.05 M, blocked with Triton-x100 and incubated with the probes. Finally, cells filled with biocytin were probed with Streptavidin Marina Blue® conjugate (Molecular Probes; absorption: 365 nm, emission: 460 nm) and observed under a fluorescent microscope with blue filter. The cells were also probed with primaries antibodies to neurofilament and glial fibrillary acidic proteins (GFAP, Molecular Probes) and subsequently visualized with green fluorescent Alexa Fluor 488 goat anti-mouse IgG (Molecular Probes; absorption 495 nm, emission 495 nm). An example of impaled, filled and double-labeled astrocyte is given in Fig. 1*C*.

Stimulation for EEG activation was achieved with bipolar electrodes placed either in the PPT (stereotaxical coordinates A0, L2-4, H-2.5) or in the BF (A15, L3-5, H-2). Usually, 1 to 3 trains of 70 stimuli at 100 Hz were sufficient to elicit a short-lasting (few seconds) EEG activation. Direct stimulation of cholinergic receptors was also obtained through iontophoretic microinjections of ACh (current pulses of 0.1 mA). For that, composed multibarrel electrodes of the type depicted in Fig. 5*A* were built. One barrel was used for the intracellular recording, another one contained ACh (1 M, pH 4) (Godfraind and al, 1971), and the third barrel was filled with NaCl (3 M, pH 4). The latter served as blank electrode during current injection in the ACh barrel, as source of control (vehicle) injection to discard the eventuality of an acidic reaction during the iontophoresis of ACh (Metherate and al, 1988) and as DC field potential electrode close to the impaled cell.

Extracellular K^+ concentrations ($[K]_o$) were measured with K^+-sensitive electrodes built as described in a previous paper (Amzica et al., 2002). Briefly, we used double-barrel pipettes in which the K^+ barrel was pretreated with dimethylchlorosilane, dried at 120^{o}C for 2 hours, and the tip filled with the K^+ ionophore I-cocktail A (Fluka). The rest of the K^+-sensitive barrel was filled with KCl (0.2 M), while the other barrel was filled with NaCl (2 M). The K^+ electrode was calibrated in solutions containing: NaCl 126 mM, KCl 2.3 mM, $NaHCO_3$ 26 mM, $MgSO_4$ 1.3 mM, $CaCl_2$ 2.4 mM, KH_2PO_4 1.2 mM, glucose 15 mM, HEPES 5 mM, thiourea 0.4 mM, and 3% dextran 70.000, pH 7.3. The K^+ concentration of the solution was adjusted between 1 and 25 mM by substituting the NaCl with KCl. The relationship between concentration and voltage was derived in accordance with the Nicolsky-Eisenmann equation (Ammann, 1986). We used only K^+-sensitive electrodes with sensitivity within the prevailing range (1 to 6 mM) better than 10 mV/mM.

Additional EEG electrodes (silver screws) fixed in the bone, and lower resistance (5-10 MΩ) glass pipettes in the cortex were used for monitoring of the EEG (AC recordings) and intracortical field potentials (DC recordings), respectively. All intracortical electrodes were kept as much as possible very close one to another and at the same cortical depth with at least one of the impaled cells. The reference electrode (Ag/AgCl) was placed in the temporal muscles of the paralyzed animal. The intracellular signals were passed through a high-impedance amplifier with an active bridge circuitry (bandwidth DC to 9 kHz; Neurodata), and together with the rest of the signals were digitized (20 kHz sampling rate) and stored for off-line analysis.

Glutamatergic AMPA/kainite receptors were blocked with a superfusion of CNQX (1 mM). The solution was delivered on a round filter paper placed over the cortical recording site (see Fig. 9*A*). Muscarinic receptors were blocked with scopolamine (0.5 mg/kg), while nicotinic receptors were blocked with mecamylamine (30 μg/kg), both injected i.v. Unless specifically mentioned, all chemicals were acquired from Sigma.

The CBF was measured by use of a laser Doppler flowmeter (Moor Instruments, USA). The probe was kept at the cortical surface close (1-2 mm) to the intracellular electrodes. A pulsatile signal indicated that the probe was sampling tissue flow. Because the device

provides a relative, not absolute, measure of flow, CBF values were calculated as a percentage of the average values during a baseline period of at least 2 min.

2.5 Results

2.5.1 Database

A total of 131 neurons and 326 glial cells were retained for the present study. Of these 81 were simultaneously recorded couples (52 neuron-glia couples, 10 neuron couples and 19 glia couples). All impaled neurons were tested with depolarizing pulses in order to elicit patterns of action potential discharges. No neurons with short action potentials and high frequency firing were recorded. Most of the neurons (83%) displayed regular, slow or fast adapting discharges. The rest of the neurons discharged in bursts. Based on this electrophysiological criterion (Connors and al, 1982, Nunez and al, 1993), we therefore assumed that all of them were excitatory neurons.

2.5.2 Activation patterns in glia

At the EEG level, electric stimulation of the PPT nucleus abolished the slow (<1 Hz) and ample oscillations that were typical for the anesthesia used here, and replaced them with an activated EEG pattern (between asterisks in Fig. 1*A*) characterized by faster and smaller waves. This behavior was in agreement with previous reports (Moruzzi and Magoun, 1949, Steriade and al, 1993a). The stimulation of the upper brainstem reticular core is expected to produce an increase in the cortical ACh release (Celesia and Jasper, 1966, Szerb, 1967). The vast majority of glial cells under PPT stimulation (143 out of 168, i.e. 85%) displayed a sustained hyperpolarization in parallel with the associated EEG activation (Fig. 1*A*). In all these cases, the glial V_m reached a level either more hyperpolarized than the inferior limit of control levels (average V_m minus the standard deviation, both calculated over a period equal to the duration of the subsequent activation; *lower dotted line* in Fig. 1*A*), or within the limits of the hyperpolarizing state of the slow oscillation. In average, the hyperpolarization reached 3.7 ± 0.86 mV (average ± SD; n = 143). This persistent hyperpolarization could be occasionally preceded by a transient depolarization during and immediately after the stimulation. In the remaining 15% cases, a sustained depolarization of the glial cells was noticed (see examples in Figs. 4 and 11).

The stimulation of the BF led to similar results: 84% of the glial cells (112 out of 133) hyperpolarized, while 16% depolarized. The average hyperpolarization was 3.2 ± 0.7 mV, but no significant difference was noted with respect to the one elicited by PPT stimulation (paired t-test, $p<0.05$). It was concluded that similar effects were induced by PPT and BF stimulation. No voltage dependence of the activating response could be established. In individual glial cells, the hyperpolarizing deflection after the activating stimulation was not larger in cells displaying a more depolarizing resting V_m.

Among glial cells responding to EEG activation with a sustained hyperpolarization, all cells that were filled with biocytin (n = 12) proved to be astrocytes (Fig. 1*C*). The cortical depth distribution of the activation pattern of impaled glia did not show any particular preference for a given cortical layer.

The prevalent hyperpolarization of glial cells during EEG activation was confirmed by intraglial recordings (n = 5) in naturally behaving animals with spontaneous sleep-waking cycles (Fig. 2*A*-*C*). The transition from slow-wave sleep (SWS) to wakefulness (W) was accompanied by a transient short-lasting depolarization, followed by a persistent hyperpolarization. When tested (n = 3), the input resistance of glia displayed increased values during wakefulness (W trace in Fig. 2*C2*) with respect to slow-wave sleep values (SWS trace).

In both chronic and acute preparations the glial hyperpolarization was paralleled by a simultaneous drop in the overall $[K^+]_o$ (Fig. 2*D*). The sleep-like pattern, dominated by a slow (<1 Hz) oscillation, produced coherent and in-phase oscillations of the $[K^+]_o$ and glial V_m (cross-correlation in Fig. 2*D2*, continuous line) with an amplitude of about 0.5-1 mM, as previously reported (Amzica and al, 2002). The activation produced an equivalent drop of the $[K^+]_o$: if the glial hyperpolarization attained the potentials reached during the "down" phase of the slow oscillation, then the K^+ values fell to the lower levels recorded during the slow oscillation. The cross-correlation between K^+ and glial V_m (broken line in Fig. 2*D2*) failed to show in the short term consistent patterns of synchrony, probably due to the diminished coherence of cortical activities during activated states.

At the same time, during the activated period, the non-filtered (DC) intracortical field potentials maintained a positive potential. Thus, during the slow sleep oscillations, the extreme values of the glial V_m and $[K^+]_o$ were in-phase, and both were in phase opposition with the polarity of the DC field potential (see also Fig. 3 in (Amzica and al, 2002)). Moreover, this relationship was kept during activation, raising the issue of the neuronal contribution to the genesis of the local field potential.

2.5.3 Glia-neuronal relationship during EEG activation

Neuron-glia couples provided a consistent pattern during both activation elicited by PPT stimulation (Fig. 3*A*) and spontaneous short-lasting activation (Fig. 3*C*): the neuronal V_m depolarized to the level of the sleep "up state" (Fig. 3, panels *B1* and *D1*, respectively), while the glial V_m hyperpolarized to the level of its sleep "down state" (Fig. 3, panels *B2* and *D2*, respectively). This evolution was consistently associated with a DC field potential that, during activation, kept with its previous sleep "down state" level (Fig. 3*A* for stimulation, and Fig. 3*B* for spontaneous activation).

The statistical analysis of this behavior relied on the peaks of V_m histograms (e.g. Fig. 3*B* and *D*). The average difference between the "up state" V_m and the activated V_m in neurons was -0.8 ± 0.1 mV (no significant difference, paired t-test). The same comparison indicated a net hyperpolarization of glia by -0.3 ± 0.1 mV that reached statistical significance ($p > 0.05$; $n = 27$) with respect to its control "down state".

In those cases where glial depolarization was elicited (25 glia with PPT stimulation and 21 glia with BF stimulation), the accompanying neuron displayed an overt depolarization with increased firing rate (Fig. 4). This behavior was consistently accompanied by a DC field potential reaching its previous sleep "up state". Thus, when both neurons and glia were depolarized by activating stimuli, intracortical DC field potentials reflected an excited network, while when glial cells were hyperpolarized by the same stimuli, the associated DC field potentials displayed the pattern of a "silent" network although neurons were in a depolarized state.

These findings critically raise the issue of the cholinergic influence on each category of cells (neurons and glia), but even more so on the reciprocal actions, non-cholinergic this time, between neurons and glia. Although this issue is extremely difficult to be dealt with *in vivo*, we attempted at intervening with locally delivered agents.

2.5.4 Iontophoretic application of ACh on glia

A first step in establishing the direct action of ACh on glial cells relied on iontophoretic application of ACh on glial cells. In all recorded glial cells (n = 12) this maneuver induced a persistent hyperpolarization (Fig. 5). The average hyperpolarization reached was 9.6 ± 2.4 mV. Given the proximity between the tip of the electrode that impaled the glia and the iontophoretic barrel (<10 μm, Fig. 5*A*) it can be assumed that most of the ejected ACh was effectively poured over the recorded glia. However, we cannot completely rule out the surrounding excitation from neurons directly stimulated by ACh. In such a case, the measured hyperpolarization should represent an underestimate of the actual induced hyperpolarization.

Indeed, similar iontophoretic applications of ACh on neurons (n = 7) disclosed a modest depolarization accompanied by a discrete resistance increase (Fig. 6), in agreement with previous reports (Krnjevic and al, 1971). In our preparations the average neuronal depolarization, calculated between the V_m histograms peaks of the depolarizing phase of the slow oscillation, was 2.4 ± 0.7 mV (range 1 to 5 mV). The resistance increase was of 0.76 ± 0.2 MΩ.

2.5.5 Input resistance and membrane capacitance of glia during EEG activation

Among glial cells responding to activation with a V_m hyperpolarization, 87 were tested with hyperpolarizing pulses (intensity 0.5 to 1 nA) in order to investigate the input resistance and capacitance of the glial membrane before and after the EEG activation. In all cases, a consistent pattern of increased resistance and diminished membrane capacitance was recorded (Fig. 7). The control average membrane resistance of glial cells was 9.7 ± 1.2

MΩ (range 8 to 12 MΩ), while their control average membrane capacitance was 12.6 ± 2.3 pF (range 7 to 16 pF).

Stimulation of either PPT or BF nuclei induced in these glial cells, in parallel with the V_m hyperpolarization, an increased membrane resistance of 44% (range 32 to 60%) and a simultaneous drop in membrane capacitance of 39% (range 22 to 56%). These variation values were calculated as post-stimulus peak vs. control average.

The neuronal membrane consistently showed an average increased membrane resistance of 21%, as compared to a control resistance of 26 ± 3.4 MΩ. Occasionally, superimposed over this response, a delayed drop in membrane resistance could be measured (see neuronal membrane resistance in Fig. 7*B*). The latter could be attributable to the activation of neighboring neurons that would activate their glutamatergic synapses toward the recorded neuron. The estimation of the neuronal capacitance did not produce reliable results: generally, the variations measured after activation were in the range of control variations (not shown), and control variations were often subject to ample voltage shifts that are common during the slow cortical oscillation (see similar results in (Amzica and Neckelmann, 1999)).

2.5.6 Muscarinic and glutamatergic components

All above-mentioned responses of glial cells to EEG activation were abolished by the muscarinic antagonist scopolamine given systemically (Fig. 8), but not by the nicotinic antagonist mecamylamine (30 μg/kg, not shown). Shortly (<5 min) after i.v. administration of scopolamine (0.5 mg/kg), the stimulation of cholinergic nuclei (PPT of BF) failed to elicit any EEG activation, and the glial depolarization/hyperpolarization was absent (compare *left* and *right* panels in Fig. 8*A*). Similarly, the increased membrane resistance prior to scopolamine application was abolished by scopolamine (Fig. 8*B*). The same behavior in the case of neurons was reported in a previous study (Steriade and al, 1993a). It is therefore obvious that the glial behavior described in the present paper is induced by the release of ACh. However, it is still not settled whether the recorded effect

(hyperpolarization/depolarization) is exerted directly on glial cells or through the bias of neurons.

In order to further discriminate this issue, we performed intracellular recordings in neurons and glia of which glutamate receptors were blocked with CNQX (Fig. 9). This was achieved by superfusing a limited area of the suprasylvian gyrus covered with filter paper with a concentrated 1 mM solution containing CNQX (see scheme in Fig. 9*A*). Intra- and extracellular recordings were obtained both from beneath and outside the soaked area. Field potentials from the cortex with blocked glutamatergic receptors (*P1* electrode in Fig. 9*B*) displayed activities of much lesser amplitude (at least 10 times) than the ones recorded at control sites (*P3* electrode). This was taken as a sign that glutamatergic transmission was impaired beneath the filter paper soaked with CNQX. A similar test was performed in the depth of the cortex. As a rule, field potentials were almost flat at the surface of the cortex and had very low amplitudes up to a depth of 1-1.2 mm, regaining control amplitude at deeper locations.

EEG activation was still seen in the CNQX area (Fig. 9*B*). Before activation, the membrane potential of neurons recorded within the perfused cortical block (n = 15) still displayed synaptic activities reminiscent of the slow sleep oscillation, however, with diminished amplitude (Fig. 9*C*). Under normal conditions, the amplitude of the slow oscillation in cortical neurons ranged from 10 to 20 mV (average 14.3 mV), while under CNQX it dropped to an average of 3.2 mV. This partial survival might reflect a partial inactivation of glutamatergic receptors, due either to the fact that CNQX perfusion had only an incomplete effect, or to the activation of other than quisqualate/kainate receptors. Similarly, the slow oscillation in glial cells (n = 23) recorded under CNQX displayed depressed amplitude (in average from 1.3 mV to 0.2 mV).

The activation maneuvers produced in all neuron-glia paired recordings (n = 15) depolarization of the neurons and clear glial hyperpolarization (Fig. 9*C*). No depolarizing components could be detected in any of the glial recordings. Thus, in situations where glutamatergic transmission was impaired, the cholinergic effect was exclusively hyperpolarizing in all glial recordings.

2.5.7 Blood flow behavior during activation

During all situations of glial cells being hyperpolarized during EEG activation, the simultaneously recorded CBF displayed an overall increase (Fig. 10). This increase reached in average a peak of 34 ± 7.2%, regardless whether it was elicited by BF or PPT stimulation. The effect of cholinergic activation on CBF was abolished by scopolamine (0.5 mg/kg i.v., Fig. 10*C*). Interestingly, during recordings where glial cells were depolarized by the stimulation of cholinergic nuclei, the CBF was always decreased (Fig. 11). The average decrease was of 47 ± 6% at the peak of the CBF response. Again, this effect was canceled by the muscarinic antagonist scopolamine. These results establish an inverse relationship between the polarization of the glial membrane and the CBF during EEG activation.

2.6 Discussion

In this study we have established the following experimental facts:

The majority of impaled cortical glial cells were hyperpolarized during states that are associated with a cholinergic activation.

The hyperpolarization of glial cells after cholinergic activation was associated with neuronal depolarization and increased CBF. Under these circumstances, the local depth field potential adopted a positive polarity.

Occasionally, glial cells were also depolarized during the cholinergic activation, in parallel with an overwhelming neuronal depolarization and decreased CBF. This was further reflected as sustained negative field potentials.

Altogether, these findings suggest that the behavior of cortical structures during active states is the outcome of a complex interaction between networks of neurons, glia and blood vessels. The common link might well be of ionic nature, of which K^+ may play a central role, but may also rely on neurotransmitters such as glutamate and/or GABA. The study of such interactions becomes strenuous even in more simple preparations, such as *in vitro* slices, because there are no clean methods to control the behavior of two of the three

ingredients that form the functional structure of the nervous tissue. This is even truer for our *in vivo* preparation.

A large body of data (reviewed in (Wainer and Mesulam, 1990, Steriade and McCarley, 1990)) suggests that the transition from slow wave sleep to wakefulness depends, among others, on cholinergic modulatory systems. Neurons releasing ACh and giving rise to ascending projections are located in two cellular aggregates PPT and laterodorsal tegmental (LDT) nuclei at the mesopontine junction and in the *nucleus basalis* (NB) of the BF. Whereas PPT-LDT ascending axons are overwhelmingly relayed by thalamocortical glutamatergic cells, NB provides the direct cholinergic innervation of the cerebral cortex (Wainer and Mesulam, 1990, Steriade and McCarley, 1990). There is also a link between mesopontine tegmental neurons and a subpopulation of cholinergic cells in the NB and surrounding areas (Jones and Cuello, 1989, Semba, 1991). Neurons of the midbrain reticular formation increase their firing rate about 15 s before the end of sleep epochs that develop into awakening and keep a higher discharge rate during wakefulness than during slow wave sleep (Steriade and al, 1982). Increased amounts of ACh were found in the cortex during activation (Celesia and Jasper, 1966, Szerb, 1967).

These anatomo-physiological evidences set the base for the delivery of ACh in the cortex during activated states. There, ACh may influence directly the activity of neurons, glia and capillaries.

The net effect of ACh on neocortical neurons is a depolarization (Krnjevic and al, 1971, Krnjevic and Reinhardt, 1979) and a change in their V_m oscillations from slow (1-5 Hz) to fast (20-40 Hz) rhythms (Metherate and al, 1992). Stimulation of the PPT/LDT nuclei, as well as spontaneous short-lasting EEG activations under anesthesia, block the slow sleep oscillation (Steriade and al, 1993a). This effect is mainly achieved through the suppression of the periodic long-lasting hyperpolarizations. Thus, the neuronal V_m during the activated periods remained at least at the same level as the one recorded during the phasic steady depolarizations of the slow oscillation (Steriade and al, 1993a). Moreover, the incidence and synchronization of fast rhythms (mainly 30-40 Hz) during the activated state on one hand and during the depolarizing phase of the slow oscillation on the other hand does not differ overtly (Steriade and al, 1996). These findings suggest that, as far as the neuronal

spontaneous firing and its impact on target neurons are concerned, there are no major differences between the periodic depolarizations during sleep and the sustained activation during wakefulness.

Glial cells possess receptors for a variety of transmitters (Murphy and Pearce, 1987) and they release neurotransmitters (Levi and Gallo, 1995). Among receptors, those for glutamate (non-NMDA) (Sontheimer and al, 1988, Monyer and al, 1991, Steinhauser and Gallo, 1996), GABA ($GABA_A$) (Bormann and Kettenmann, 1988, MacVicar and al, 1989, Rosier and al, 1993), and ACh (Van Der Zee and al, 1993), are of particular interest in the present study. Glutamate, an ubiquitous transmitter in the central nervous system, depolarizes glia through receptors similar to the ones of the neurons (Bowman and Kimelberg, 1984, Kettenmann and Schachner, 1985), and direct chemical synapses between neurons and glia have been found (Bergles and al, 2000). Activation of $GABA_A$ receptors in glia opens Cl^- channels and is responsible for glial depolarization (Bowman and Kimelberg, 1984, Kettenmann and Schachner, 1985). Thus, the depolarizing responses noted occasionally in this study might be provoked by the glutamate and/or GABA release from neurons that were activated by ACh.

Our study, especially when using iontophoretic application of ACh and blockage of glutamatergic receptors, emphasizes the hyperpolarizing response of glia during activation. This was in line with a previous *in vitro* study in which the application of ACh on astrocytes usually produced a long lasting hyperpolarization (Hosli and Hosli, 1993, Hosli and al, 1988). The direct effect of ACh on cortical glia is achieved on both protoplasmatic and fibrous astrocytes mainly through muscarinic receptors (Van Der Zee and al, 1989). Scopolamine was indeed effective in blocking the cholinergic response in our glial cells (Fig. 8). Nicotinic receptors on astrocytes were also found in autoradiographic studies on explant cultures, although with lesser incidence than muscarinic receptors (Hosli and al, 1988) and are thus expected to play a negligible role (Walz, 1995). This was also the case of our recorded glial cells that did not show any sensitivity to the nicotinic antagonist mecamylamine.

We can therefore conclude that the cholinergic activation of the cortex has a twofold effect on glia: one direct and hyperpolarizing, through muscarinic receptors situated on the glial

membrane, and the other indirect and depolarizing, through the activation of neurons that further release glutamate (in the case of excitatory neurons) or GABA (in the case of interneurons) on neighboring glia. The excitation of surrounding neurons might also provoke release of K^+ by these neurons that should equally have a depolarizing effect on glia. This would be in agreement with the behavior of putative glial cells in the hippocampus (Casullo and Krnjevic, 1987). The global effect seems to lean, in most of the cases, towards a resulting hyperpolarization of the glia. In those cases where a net depolarization of glia was recorded, we suggest that the combined glutamatergic/GABAergic/K^+ action of neighboring neurons overwhelmed the direct cholinergic action.

At first sight this behavior might be difficult to explain, especially because, in glia, it is associated with increased membrane resistance and decreased membrane capacitance (Fig. 7). The former feature might result from the muscarinic reduction of a resting K^+ conductance of cortical glia and should diminish the transfer of cations across the glial membrane. The capacitance reduction could reflect shrinkage of the glial membrane and/or closing of gap junctions (Amzica and Neckelmann, 1999). In the latter case, one would expect impaired spatial buffering across the glial syncytium during the activating process. It has been proposed that synchronous activities like those present during sleep (e.g. the slow, <1 Hz, sleep oscillation), and even more so hypersynchronous epileptic discharges are supported by the presence of a functional glial syncytium (Amzica and al, 2002). Therefore, the relative locally restricted synchronization of fast activities during activated states (Steriade and Amzica, 1996, Steriade and al, 1996) might be explained by a relatively disconnected glial network.

Alternatively, we should also consider the variations of the $[K^+]_o$ (Fig. 2) and the behavior of blood vessels as a result of the cholinergic stimulation in the cortex (Figs. 10-11). By increasing the cerebral glucose metabolism (Maquet, 1997) and blood flow (Madsen and Vorstrup, 1991, Braun and al, 1997, Elhusseiny and Hamel, 2000, Tong and Hamel, 2000), the activation might produce an increased washout of the extracellular K^+. The latter hypothesis corroborates with the increased $[K^+]_o$ after reduction of the blood flow by occlusion of the carotid artery (Harris and Symon, 1984) and during those activations that

depolarized glia (Fig. 11). In other terms, the glial hyperpolarization might also reflect a depleted $[K^+]_o$.

A third alternative could rely on an ATP-dependent mechanism as follows: increased metabolic demands during EEG activation might hyperpolarize glial cells through ATP-sensitive K^+ channels (Brockhaus and Deitmer, 2000), which also would contribute to the inhibition of gap junction communication (Velasco and al, 2000), in line with the decreased glial capacitance reported in Fig. 7. This hypothesis needs, however, further testing because the existence of ATP-sensitive K^+ channels have not yet been described in cat cortical glia, and they seem to undergo developmental downregulation (Brockhaus and Deitmer, 2000).

The combination of the two non-exclusive mechanisms of action (neurotransmitter- and blood flow-mediated) could further explain the lack of voltage-dependency of the glial hyperpolarization.

2.6.1 Consequences of the glial/vascular behavior during cholinergic activation

The unfiltered (DC) recording of local depth field potentials produced an interesting finding: their outcome is influenced not only by the neuronal activity, but also by the polarization of the glial membranes (Figs. 3-4), which in turn depend on the K^+ siphoning through capillaries. This opens new perspectives for the genesis of steady potentials in the EEG.

Thus, the understanding of mechanisms that rule conscious behavior must rely on a more complex approach taking into consideration tripartite interactions between neurons, glial cells and blood supply because none of these three elements can modulate its activity without influencing and undergoing the reciprocal influence of the other two.

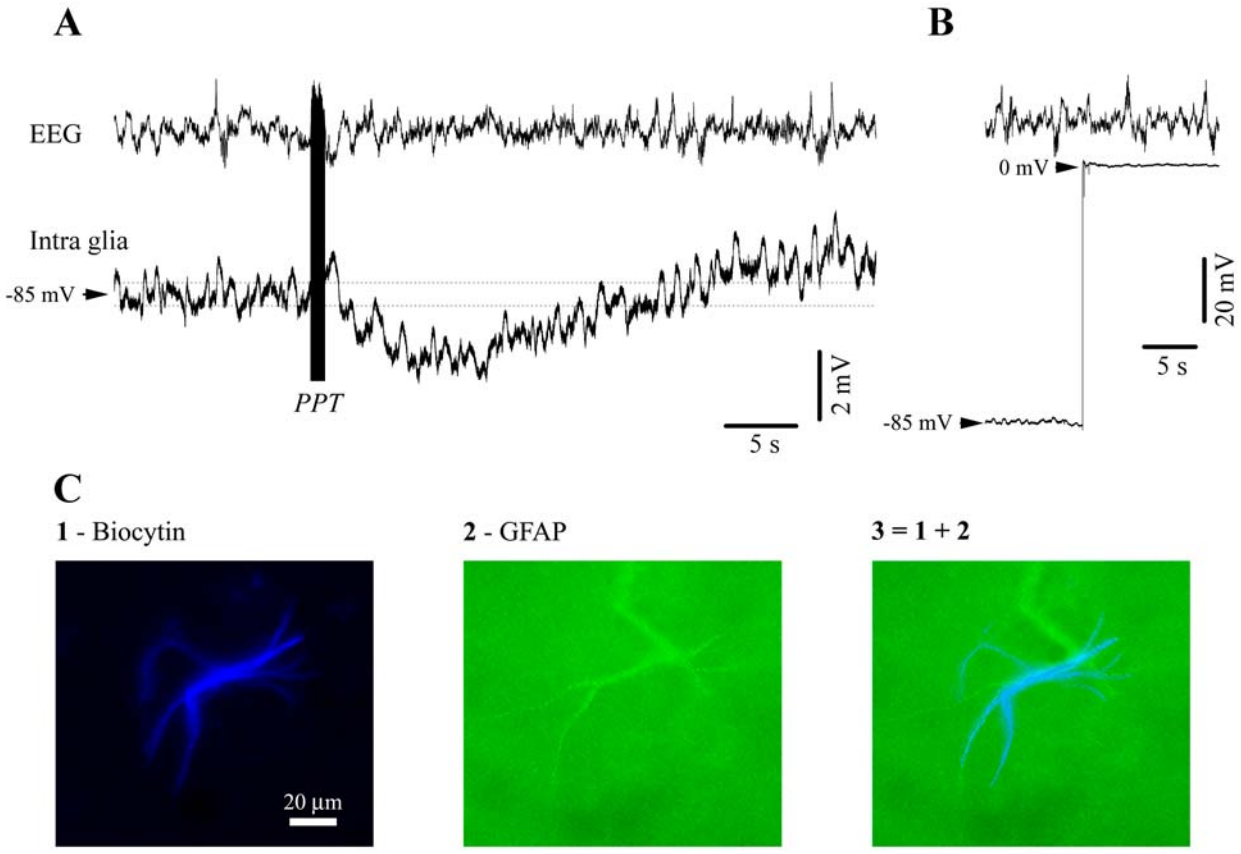
A
EEG
Intra glia
-85 mV
PPT
2 mV
5 s
B
0 mV
20 mV
5 s
-85 mV
C
1 - Biocytin
2 - GFAP
3 = 1 + 2
20 µm

Figure 1: Hyperpolarizing responses in astrocytes after PPT activation.

A, Intraglial (microelectrode filled with biocytin) and EEG recording from a cat under ketamine & xylazine anesthesia. The intracellular recording was performed in area 5 and the EEG electrode (screw in the bone) was placed just anterior to the intracellular pipette. The stimulation of the PPT nucleus (100 stimuli at 100 Hz) elicited a prolonged hyperpolarization. **B**, At the end of the recording, the intracellular electrode was withdrawn from the glia for verification of the real V_m. **C**, Anatomical verification of the glia recorded in **A** and **B**. *Panel 1* displays the shape of an astrocyte, *panel 2* the same cell verified for reactivity to GFAP, and *panel 3* contains the superimposition of the previous 2 panels. In this and all subsequent figures potentials are presented with positivity upwards.

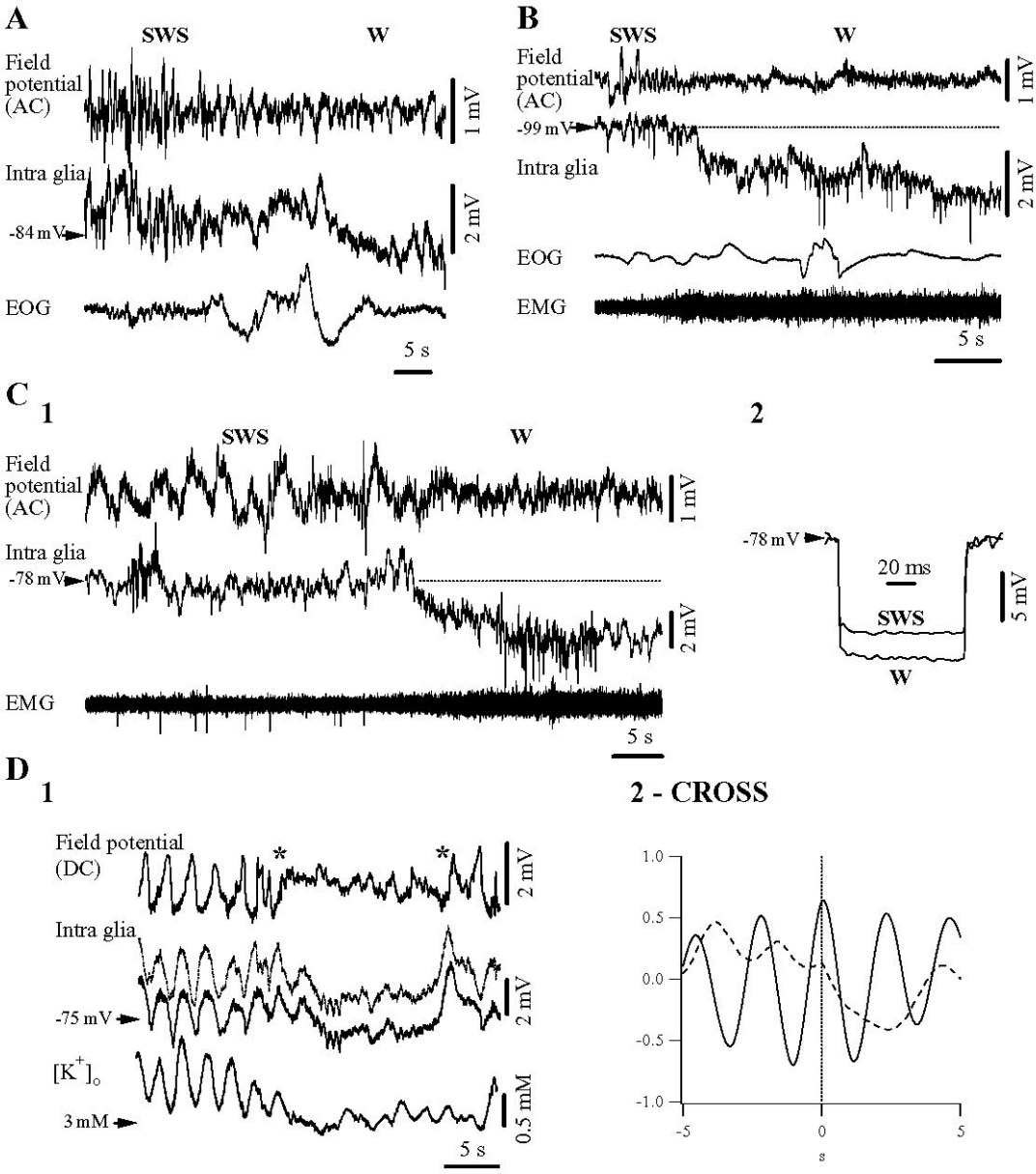
A
SWS
W
Field potential (AC)
1 mV
Intra glia
-84 mV
2 mV
EOG
5 s
B
SWS
W
Field potential (AC)
1 mV
-99 mV
Intra glia
2 mV
EOG
EMG
5 s
C
1
SWS
W
Field potential (AC)
1 mV
Intra glia
-78 mV
2 mV
EMG
5 s
2
-78 mV
20 ms
5 mV
SWS
W
D
1
Field potential (DC)
2 mV
Intra glia
-75 mV
2 mV
[K+]o
3 mM
0.5 mM
5 s
2 - CROSS
1.0
0.5
0.0
-0.5
-1.0
-5
0
5
s

Figure 2: Glial hyperpolarization in a chronically implanted cat during natural transition between slow wave sleep (SWS) and wakefulness (W).

A-C, Intraglial, AC field potential, electrooculogram (EOG) and electromyogram (EMG) during spontaneous activation. Awakening is marked by suppression of ample slow waves and eye opening (two deflections). In parallel the intracellular recording displays a sustained hyperpolarization. **D1**, Simultaneous recording of a glia and of the extracellular K^+ concentration ($[K^+]_o$) during a brief period of spontaneous activation (between *asterisks*). Note simultaneous glial hyperpolarization and $[K^+]_o$ decrease. At the same time, the DC field potential measured at close distance evolves toward a positive value. **D2**, Cross-correlations between intraglial potentials and $[K^+]_o$ performed over two 30 s periods during SWS (continuous line) and W (broken line).

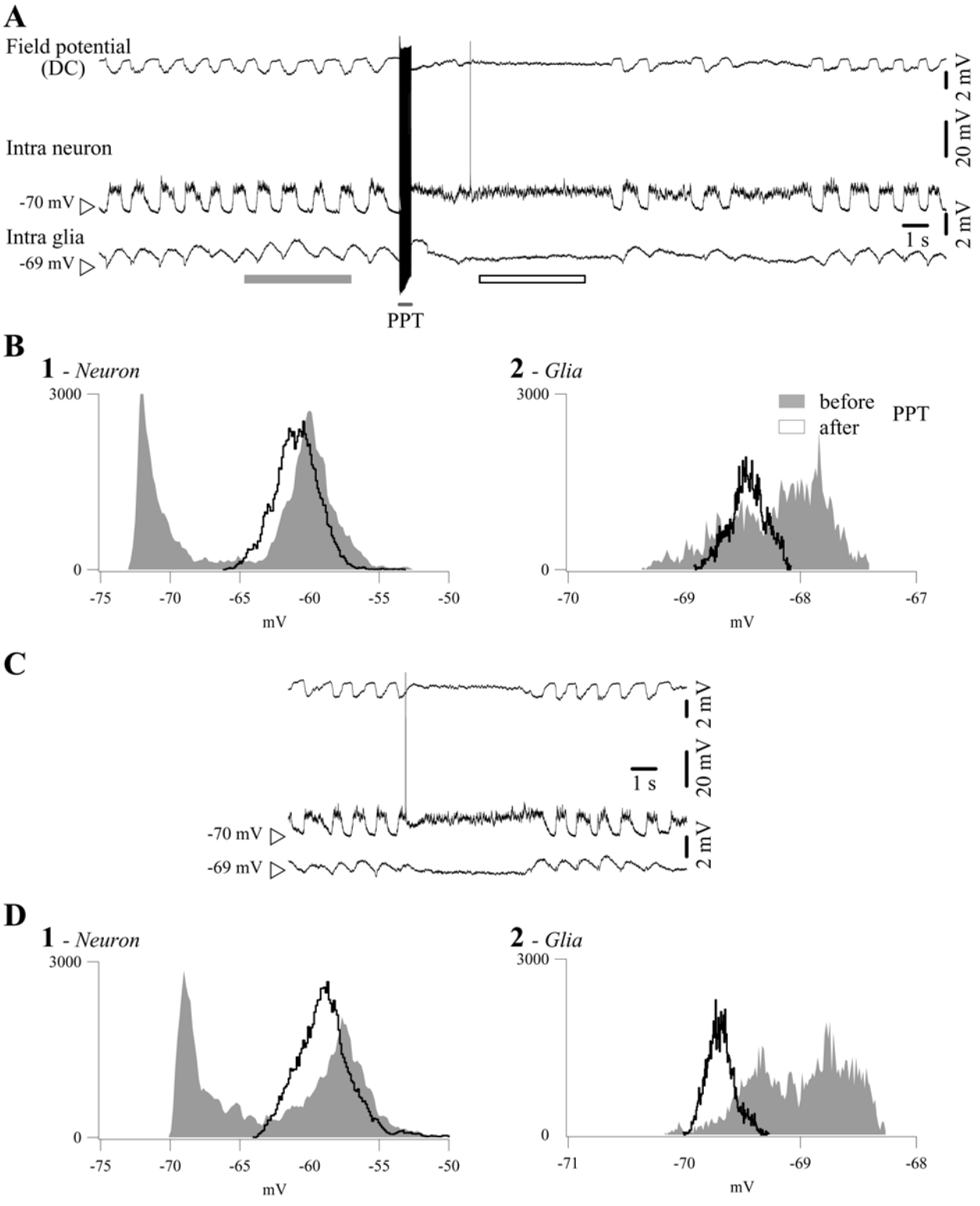
A
Field potential
(DC)
Intra neuron
-70 mV
Intra glia
-69 mV
20 mV 2 mV
2 mV
1 s
PPT
B
1 - Neuron
2 - Glia
3000
0
-75 -70 -65 -60 -55 -50
mV
-70 -69 -68 -67
before
after
PPT
C
2 mV
20 mV
1 s
-70 mV
-69 mV
2 mV
D
1 - Neuron
2 - Glia
3000
0
-75 -70 -65 -60 -55 -50
mV
-71 -70 -69 -68

Figure 3: Comparison between electrically elicited and spontaneously occurring activation in a pair of simultaneously impaled neuron and glia in a cat under ketamine & xylazine anesthesia.

A, Sequence of slow (<1 Hz) oscillation, PPT activation and return to slow oscillation. During the sustained neuronal depolarization glia is hyperpolarized and the DC field potential assumes rather positive values. **B**, Histograms of neuronal (*panel 1*) and glial (*panel 2*) V_m during the slow oscillation (*in gray*) and during activation (*black trace*). Histograms were calculated over the respective underlined epochs in **A**. They illustrate the incidence of different values of V_m, sampled at 20 kHz, over periods indicated by bar below traces. Note the bimodal histograms during sleep and the unimodal histogram after activation, as well as the opposite evolution of glial and neuronal V_m (glia hyperpolarizes, neuron depolarizes). **C**, Similar pattern of activity in the same double intracellular recording during a period of spontaneous activation of the EEG. Periods within squares are expanded at right (*panels 2* and *3*). **D**, Histograms from equivalent time periods before and after activation.

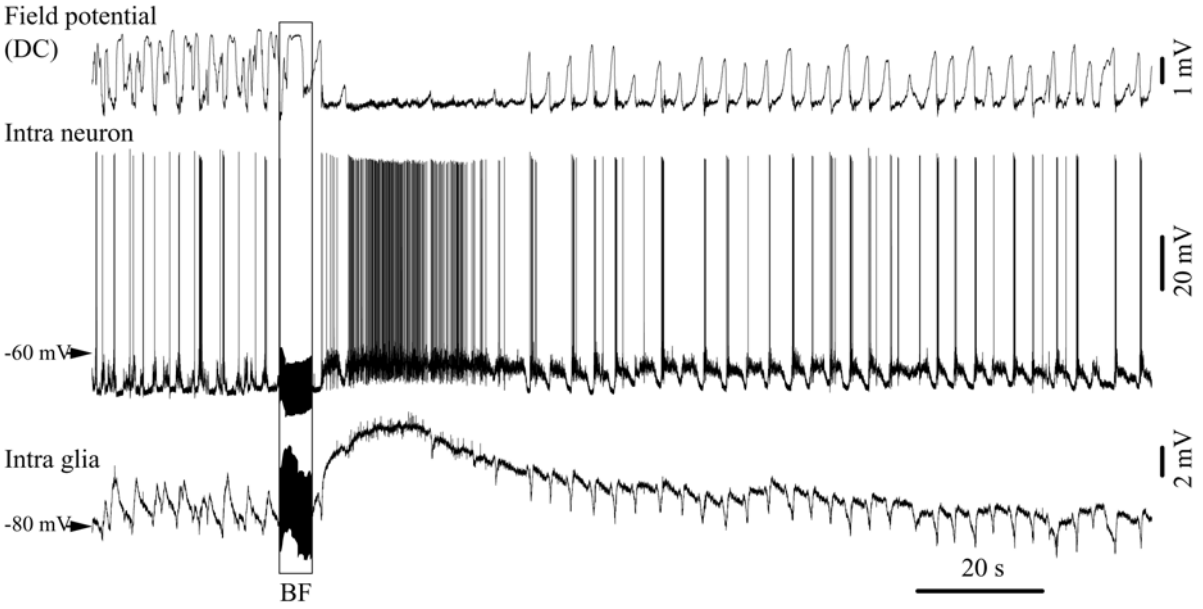
Field potential
(DC)
1 mV
Intra neuron
20 mV
-60 mV
Intra glia
2 mV
-80 mV
20 s
BF

Figure 4: Double intracellular recording (neuron-glia pair) in the suprasylvian gyrus displaying glial depolarization during BF-elicited activation.

In this case, the glial depolarization is associated with a neuronal depolarization, as reflected by the increased discharge of action potentials. During such activations, DC field potentials assumed sustained negative values.

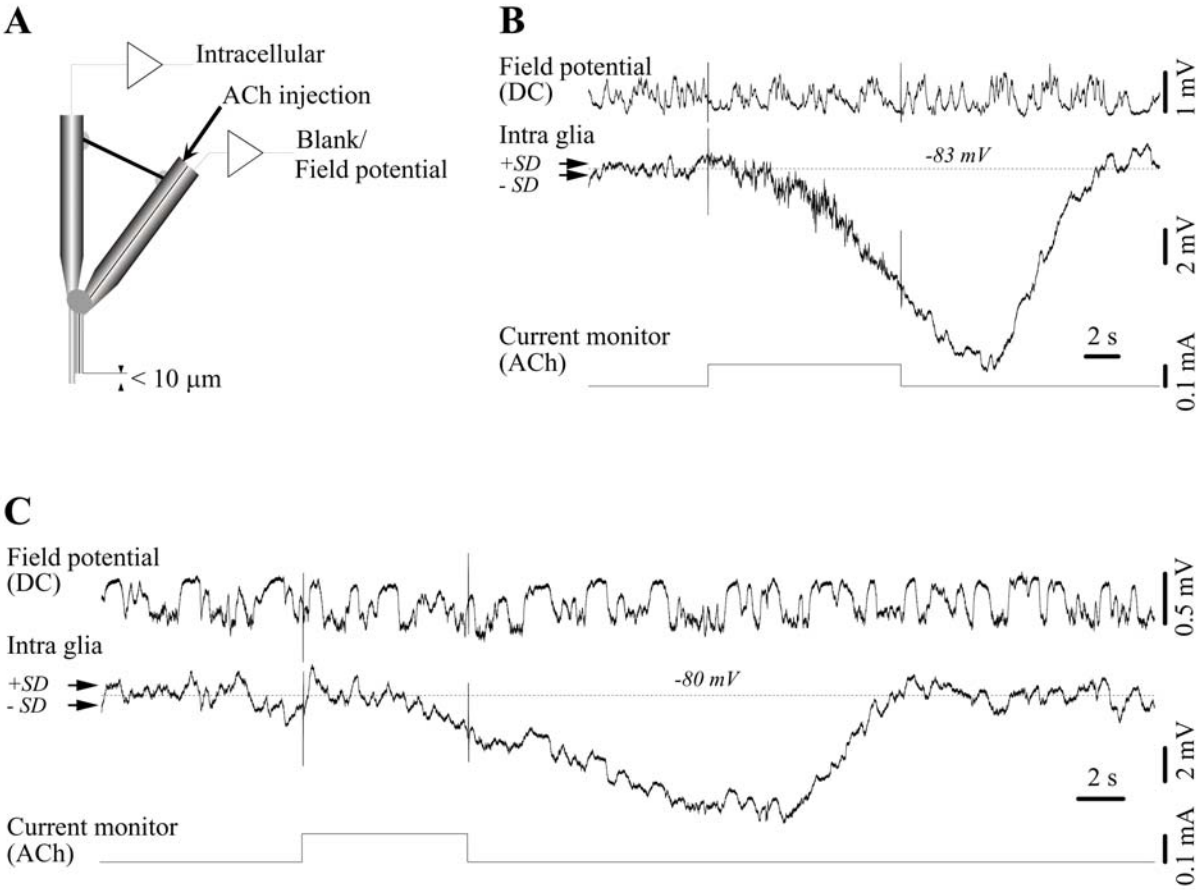
A
Intracellular
ACh injection
Blank/
Field potential
< 10 µm
B
Field potential
(DC)
1 mV
Intra glia
+SD
- SD
-83 mV
2 mV
Current monitor
(ACh)
2 s
0.1 mA
C
Field potential
(DC)
0.5 mV
Intra glia
+SD
- SD
-80 mV
2 mV
2 s
Current monitor
(ACh)
0.1 mA

Figure 5: Iontophoretic application of ACh induced glial hyperpolarization.

Iontophoretic application of ACh induced glial hyperpolarization. **A**, Scheme of the iontophoretic electrodes used in this study. They resulted from attaching together two microelectrodes: the vertical one, serving for intracellular impalements, and the crooked one, a double barrel pipette containing ACh in one barrel and NaCl in the other one. The tip of the iontophoretic barrels of the compound electrode, assembled under a microscope, was about 10 μm above the intracellular recording tip. **B** and **C**, Two different glial cells undergoing iontophoretic application of ACh. The current monitor below the traces indicates the intensity (0.1 mA) and duration of ACh ejection. The dotted lines indicate the average control V_m, and the two arrows the limits of the standard deviation (SD). The field potential was not affected by the iontophoretic injection, suggesting that the cholinergic effect did not activate many cells.

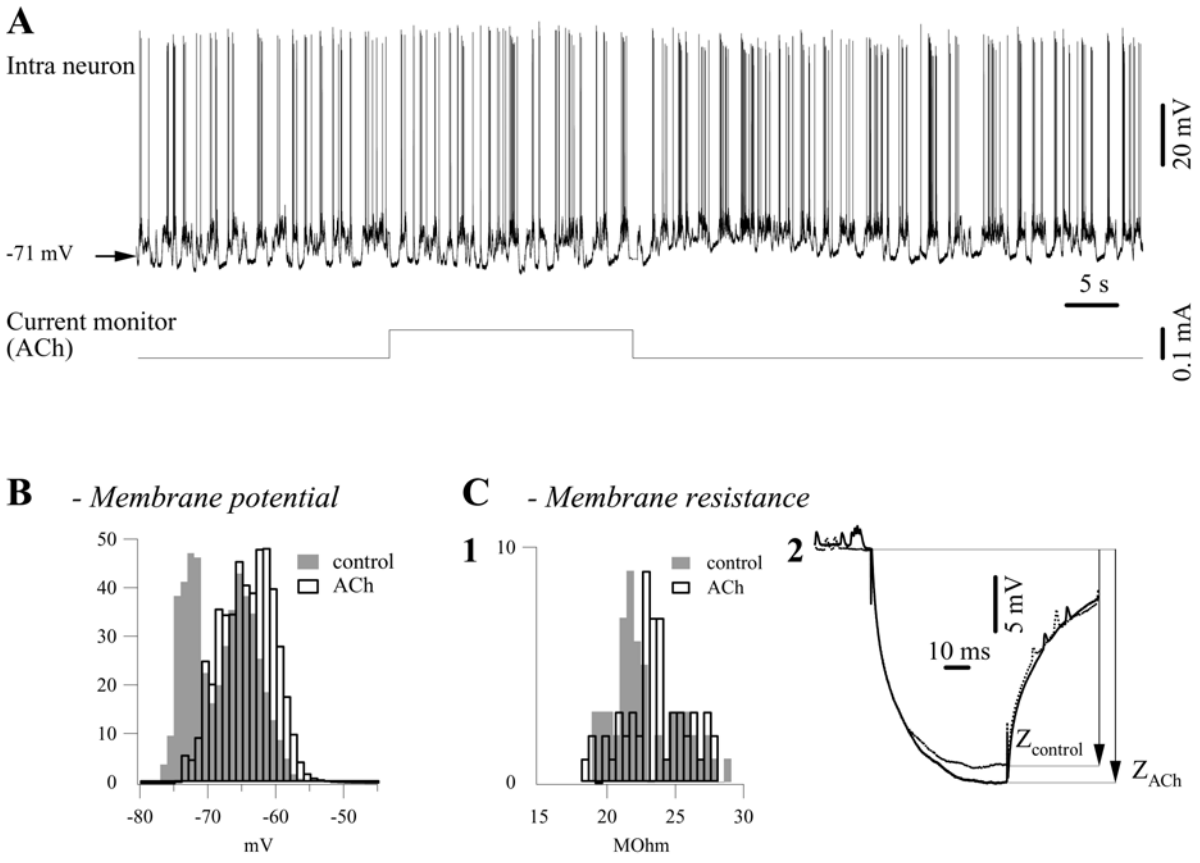
A
Intra neuron
-71 mV
20 mV
5 s
Current monitor
(ACh)
0.1 mA
B - Membrane potential
control
ACh
50
40
30
20
10
0
-80
-70
-60
-50
mV
C - Membrane resistance
1
10
0
control
ACh
15
20
25
30
MOhm
2
5 mV
10 ms
Z control
Z ACh

Figure 6: Iontophoretic application of ACh on neuron.

A, Similar iontophoretic application of ACh (0.1 mA injection current) on neurons induced depolarization. **B**, V_m histogram calculated over equal periods of time before (in *gray*) and after (*white bars*) the application of ACh. Note clear depolarization as well as suppression of the bimodal, oscillatory pattern, after ACh iontophoresis. **C**, Neuronal input resistance before and after ACh application. *Panel 1*, histogram from individual hyperpolarizing pulses, *panel 2*, average pulse responses. Both show increased membrane resistance after iontophoresis.

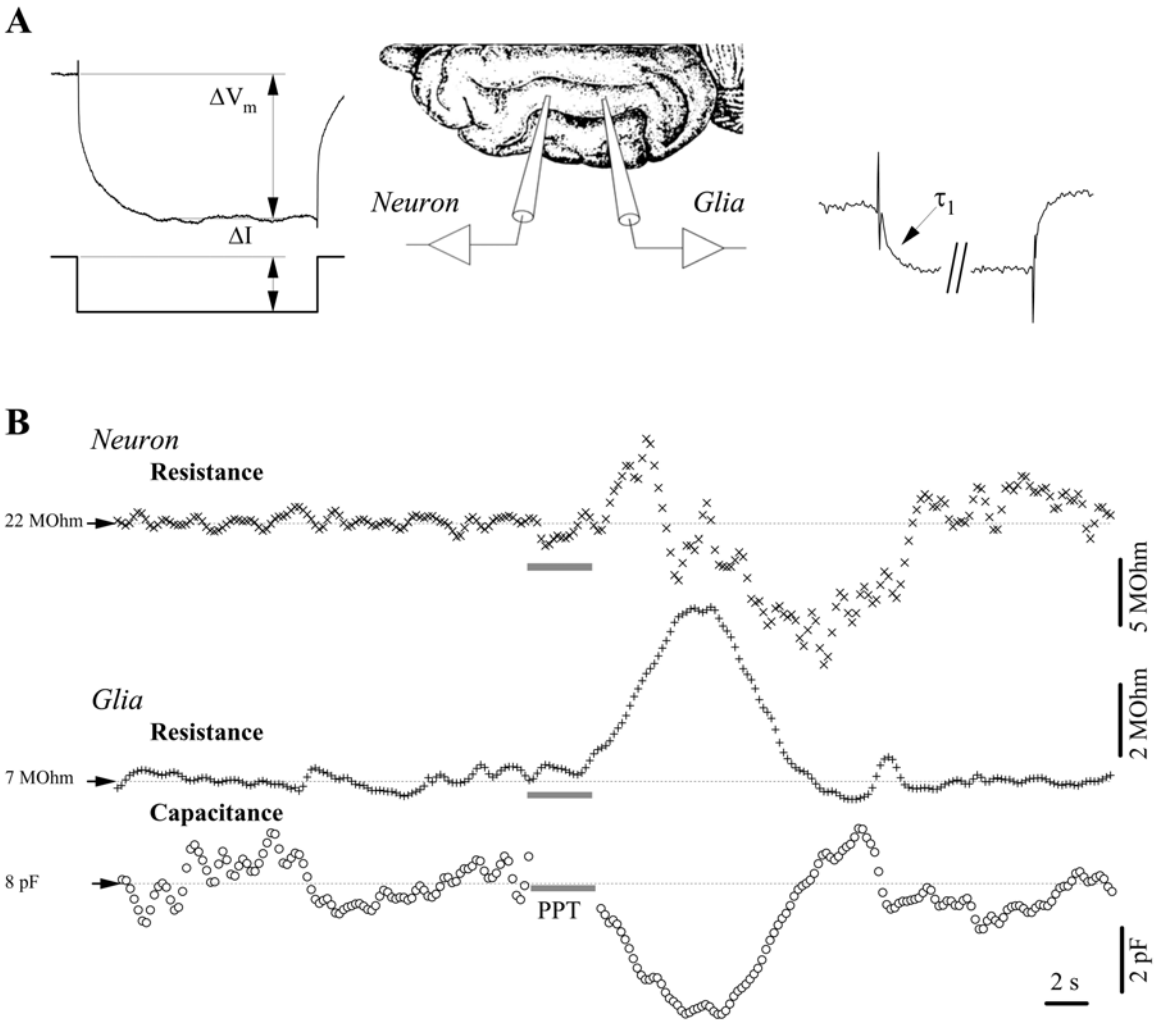
A
ΔV_m
ΔI
Neuron
Glia
τ_1
B
Neuron
Resistance
22 MOhm
5 MOhm
Glia
Resistance
7 MOhm
2 MOhm
Capacitance
8 pF
PPT
2 pF
2 s

Figure 7: Membrane resistance and capacitance during PPT activation in a simultaneously impaled neuron-glia pair.

A, Measurement principle: hyperpolarizing pulses of fixed intensity (ΔI) were delivered at high rate (5 Hz) in both cells. The voltage deflection after the reaching of the plateau (ΔV_m) served to the calculation of both resistances. Additionally, the charging curve of the glial response produced the time constant of the glia membrane (τ_1), and further the glial membrane capacitance. **B**, Dynamic evolution of the neuronal membrane resistance and of the glial membrane resistance and capacitance. The stimulation of the PPT at the *horizontal gray bar*. Note increase-decrease sequence in the neuronal resistance recording, and increased membrane resistance in glia, in parallel with decreased capacitance.

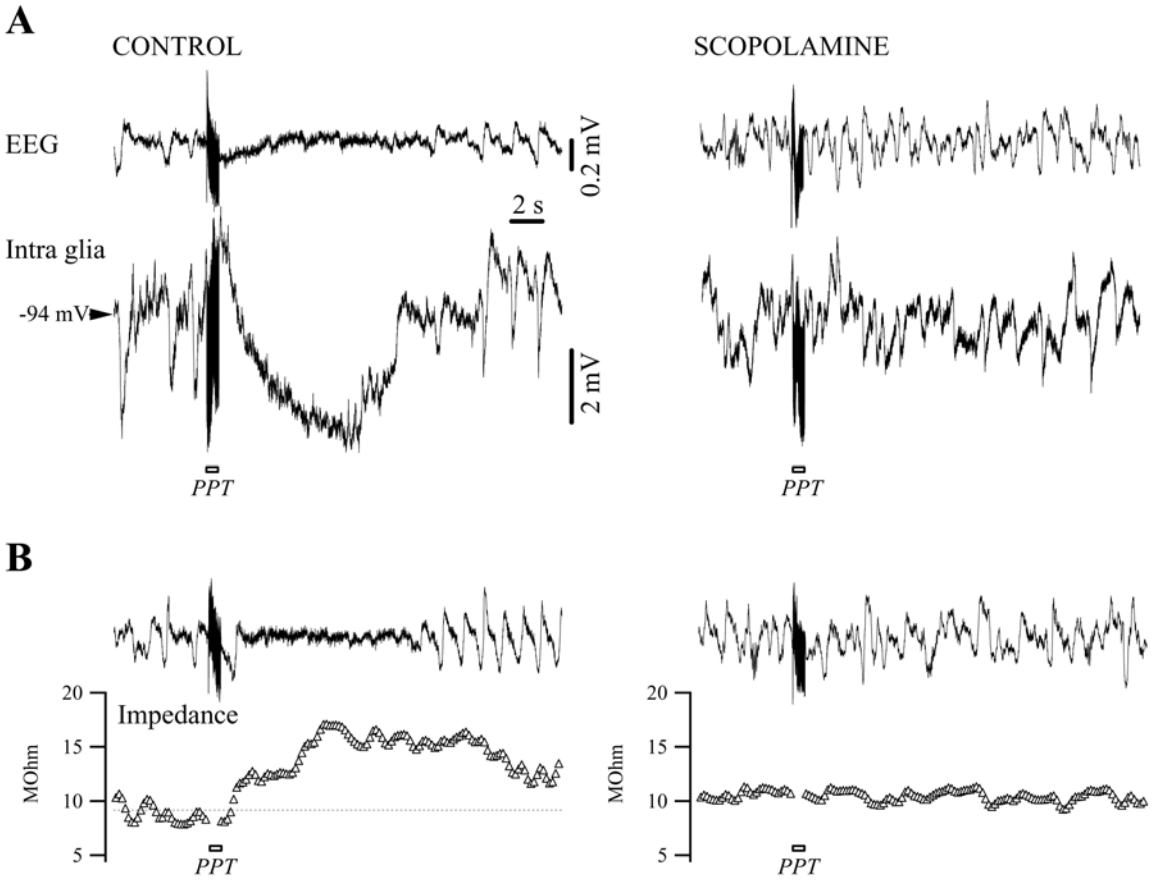
A
CONTROL
SCOPOLAMINE
EEG
0.2 mV
2 s
Intra glia
-94 mV
2 mV
PPT
PPT
B
Impedance
MOhm
20
15
10
5
PPT
MOhm
20
15
10
5
PPT

Figure 8: Muscarinic antagonist scopolamine abolishes V_m hyperpolarization and membrane resistance increase in glia.

A, Control recording in a glia before (*left*) and after (*right*) systemic application of scopolamine (0.5 mg/kg). The hyperpolarization elicited with PPT stimulation under control conditions disappears after blockage of muscarinic receptors. **B**, Input resistance modification in the same glia in control conditions (*left*) is canceled after scopolamine application (*right*).

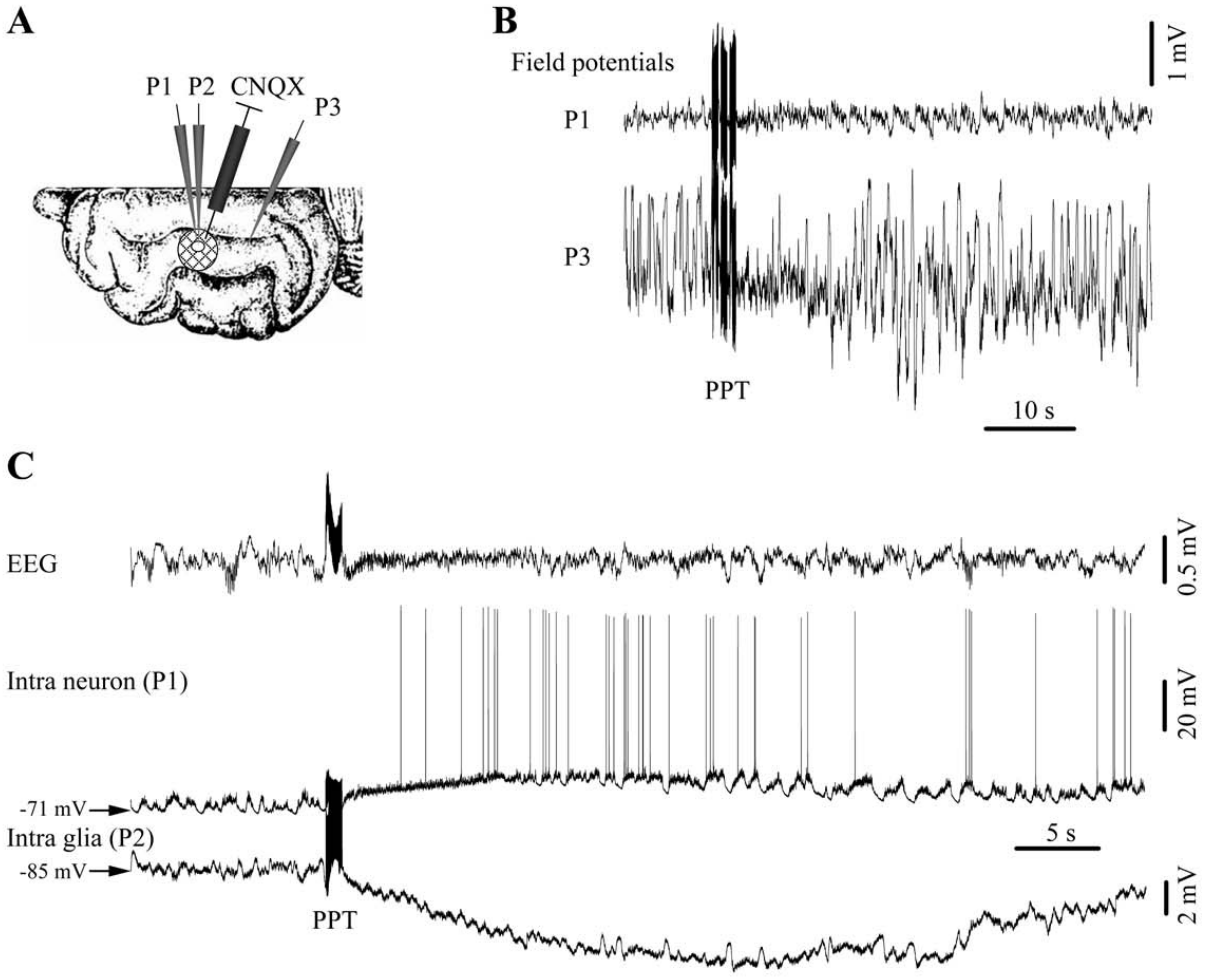
A
P1
P2
CNQX
P3
B
Field potentials
P1
P3
PPT
1 mV
10 s
C
EEG
0.5 mV
Intra neuron (P1)
20 mV
-71 mV
Intra glia (P2)
-85 mV
5 s
PPT
2 mV

Figure 9: Cholinergic effect after blockage of kainate/quiscalate glutamatergic receptors with CNQX.

A, Location of the recording electrodes in the suprasylvian gyrus. A round (~4 mm diameter) filter paper patch was placed over the cortex and continuously perfused with CNQX from a Hamilton syringe. A Whole in the patch allowed the insertion of two intracellular pipettes (*P1* and *P2*). An extra DC field potentials pipette (*P3*) was inserted at some distance (>10 mm) from the filter paper. **B**, Reduced amplitude of the field potentials measured below the CNQX soaked area (*P1*) with respect to the control microelectrode (*P3*). **C**, PPT activation of a neuron-glia pair recorded in the CNQX-inactivated area. Note depolarizing response in the neuron and exclusive hyperpolarizing response in the glial cell.

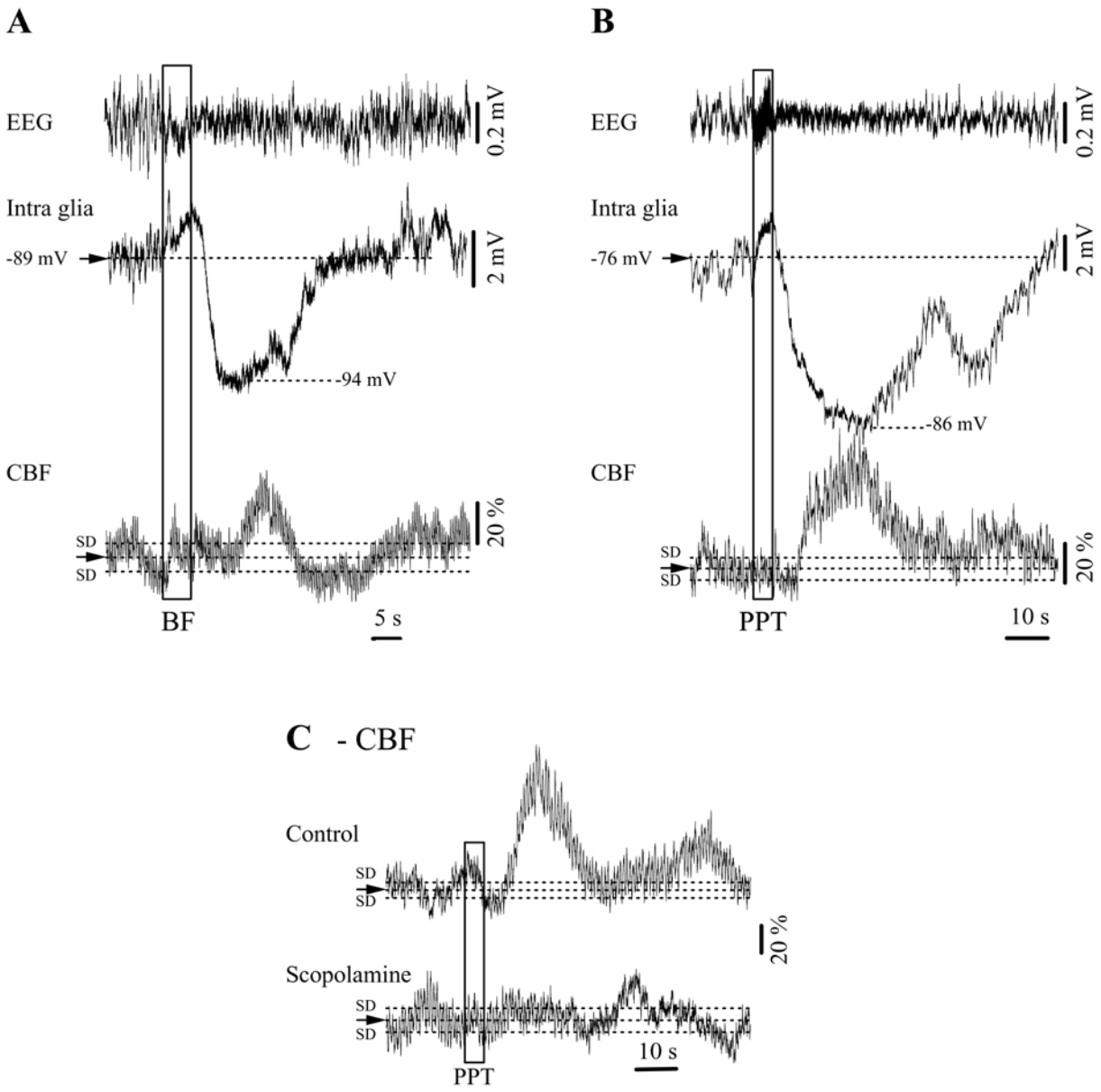
A
EEG
0.2 mV
Intra glia
-89 mV
2 mV
-94 mV
CBF
20 %
SD
SD
BF
5 s
B
EEG
0.2 mV
Intra glia
-76 mV
2 mV
-86 mV
CBF
20 %
SD
SD
PPT
10 s
C - CBF
Control
SD
SD
20 %
Scopolamine
SD
SD
10 s
PPT

Figure 10: Cerebral blood flow (CBF) in association with glial hyperpolarizing responses to cerebral activation.

Regardless of the stimulation site, hyperpolarizing responses from glial cells to BF stimulation (**A**) or PPT stimulation (**B**) were always associated with transient increases of the CBF. **C**, These responses were abolished by the muscarinic antagonist scopolamine.

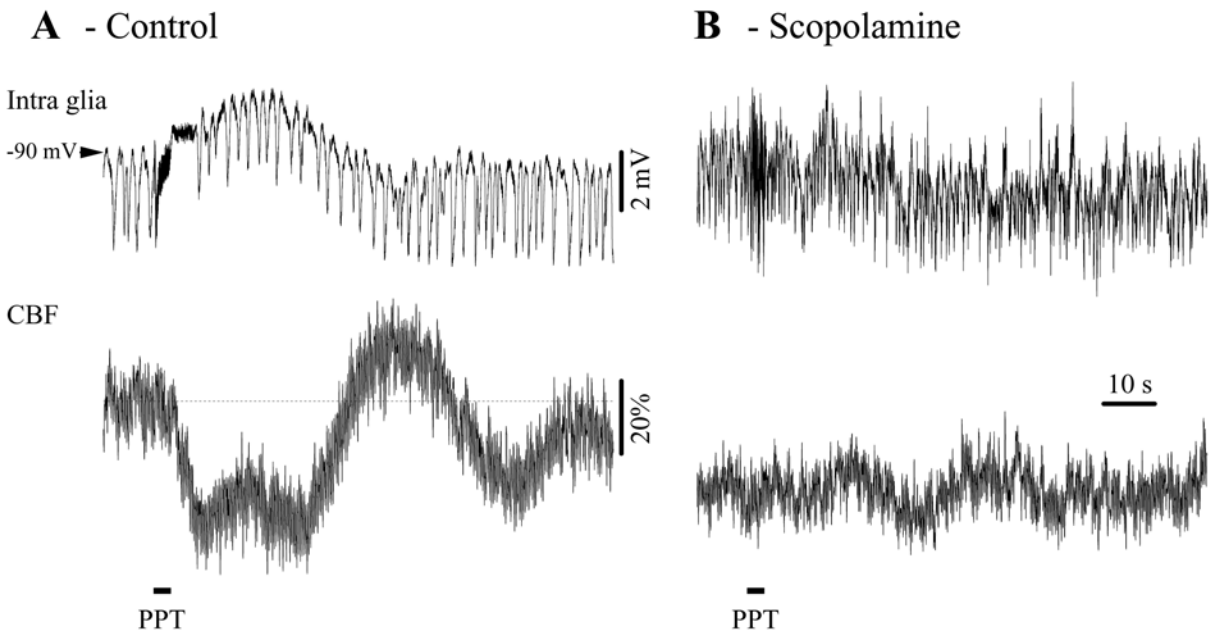
A - Control
B - Scopolamine
Intra glia
-90 mV
2 mV
CBF
20%
10 s
PPT
PPT

Figure 11: CBF in association with glial depolarizing responses to cerebral activation.

A, Glial depolarization after PPT stimulation was always associated with decreased CBF.

B, This effect was antagonized by scopolamine.

3. Conclusion

Les expériences faites chez l'animal sous anesthésie ou naturellement endormi ont démontré la capacité des cellules gliales à s'hyperpolariser lorsque les systèmes ascendants cholinergiques s'activent. Toutefois, l'étude des récepteurs gliaux *in vivo* est beaucoup plus complexe qu'en culture ou *in vitro* étant donné l'intégrité de tout le réseau cortical. Ainsi, tel qu'il a été observé dans un contexte de transition évoquée du sommeil à ondes lentes vers l'éveil, la stimulation du PPT ou du BF ne résulte pas d'une libération d'ACh seulement. Elle peut être également glutamatergique et/ou GABAergique. De plus, l'effet de la stimulation n'est pas unique sur les cellules au niveau du cortex. Néanmoins, l'application ionotophorétique d'ACh seul cause une hyperpolarisation des glies. De plus, l'hyperpolarisation a aussi pu être observée chez le chat naturellement endormi et la majorité des cellules enregistrées chez le chat sous anesthésie ont démontré une hyperpolarisation lorsque le neurone n'augmente pas de fréquence de décharge. L'hyperpolarisation est accompagnée d'une diminution du K^+ extracellulaire et d'une augmentation du débit sanguin cérébral. Également, la résistance membranaire de la glie augmente, alors que sa capacitance diminue.

Sans démontrer une action directe de l'ACh sur les glies, nos résultats mettent en évidence la participation de la glie et des vaisseaux sanguins dans l'activation de l'EEG. Jusqu'à présent, les mécanismes impliquant les systèmes ascendants cholinergiques sont entièrement basés sur les circuits neuronaux. Or, nos observations ont démontré que les glies et les vaisseaux sanguins devraient être intégrés dans la représentation des mécanismes impliquant les états de vigilance. Par leur capacité à maintenir l'équilibre du milieu extracellulaire en récupérant les ions de K^+, les glies et les vaisseaux sanguins influencent l'activité neuronale. De la même manière, ils pourraient influencer le phénomène d'attention pendant l'éveil et joueraient donc un rôle dans l'état de conscience.

De plus, étant donné que les glies exercent une action globale sur les neurones, nous pourrions investiguer la participation de la glie et la vascularisation dans la genèse de l'EEG. Il serait intéressant d'établir un profil d'EEG cortical selon la distribution laminaire des neurones, des glies et de la vascularisation et de déterminer leur contribution respective dans la génération de l'EEG.

Bibliographie

Bibliographie

Achermann P, Borbely AA (1997) Low-frequency (< 1 Hz) oscillations in the human sleep electroencephalogram. Neuroscience 81: 213-222.

Ammann D (1986) Ion sensitive microelectrodes. Berlin: Springer.

Amzica F, Massimini M (2002) Glial and neuronal interactions during slow wave and paroxysmal activities in the neocortex. Cereb Cortex 12: 1101-1113.

Amzica F, Massimini M, Manfridi A (2002) Spatial buffering during slow and paroxysmal sleep oscillations in cortical networks of glial cells in vivo. J Neurosci 22: 1042-1053.

Amzica F, Neckelmann D (1999) Membrane capacitance of cortical neurons and glia during sleep oscillations and spike-wave seizures. J Neurophysiol 82: 2731-2746.

Amzica F, Steriade M (1995) Short- and long-range neuronal synchronization of the slow (< 1 Hz) cortical oscillation. J Neurophysiol 73: 20-38.

Amzica F, Steriade M (1997) The K-complex: its slow (<1-Hz) rhythmicity and relation to delta waves. Neurology 49: 952-959.

Amzica F, Steriade M (1998a) Cellular substrates and laminar profile of sleep K-complex. Neuroscience 82: 671-686.

Amzica F, Steriade M (1998b) Electrophysiological correlates of sleep delta waves. Electroencephalogr Clin Neurophysiol 107: 69-83.

Amzica F, Steriade M (2000) Neuronal and glial membrane potentials during sleep and paroxysmal oscillations in the neocortex. Journal of Neuroscience 20: 6648-6665.

Araque A, Li N, Doyle RT, Haydon PG (2000) SNARE protein-dependent glutamate release from astrocytes. J Neurosci 20: 666-673.

Araque A, Martin ED, Perea G, Arellano JI, Buno W (2002) Synaptically released acetylcholine evokes Ca2+ elevations in astrocytes in hippocampal slices. J Neurosci 22: 2443-2450.

Araque A, Parpura V, Sanzgiri RP, Haydon PG (1999) Tripartite synapses: glia, the unacknowledged partner. Trends Neurosci 22: 208-215.

Barres BA, Barde Y (2000) Neuronal and glial cell biology. Curr Opin Neurobiol 10: 642-648.

Barres BA, Chun LL, Corey DP (1990) Ion channels in vertebrate glia. Annu Rev Neurosci 13: 441-474.

Bekar LK, Walz W (1999) Evidence for chloride ions as intracellular messenger substances in astrocytes. J Neurophysiol 82: 248-254.

Beldhuis HJ, Everts HG, Van Der Zee EA, Luiten PG, Bohus B (1992) Amygdala kindling-induced seizures selectively impair spatial memory. 2. Effects on hippocampal neuronal and glial muscarinic acetylcholine receptor. Hippocampus 2: 411-419.

Bergles DE, Roberts JD, Somogyi P, Jahr CE (2000) Glutamatergic synapses on oligodendrocyte precursor cells in the hippocampus. Nature 405: 187-191.

Bezzi P, Carmignoto G, Pasti L, Vesce S, Rossi D, Rizzini BL, Pozzan T, Volterra A (1998) Prostaglandins stimulate calcium-dependent glutamate release in astrocytes. Nature 391: 281-285.

Bezzi P, Volterra A (2001) A neuron-glia signalling network in the active brain. Curr Opin Neurobiol 11: 387-394.

Bignami A, Eng LF, Dahl D, Uyeda CT (1972) Localization of the glial fibrillary acidic protein in astrocytes by immunofluorescence. Brain Res 43: 429-435.

Bormann J, Kettenmann H (1988) Patch-clamp study of gamma-aminobutyric acid receptor Cl- channels in cultured astrocytes. Proc Natl Acad Sci U S A 85: 9336-9340.

Bowman CL, Kimelberg HK (1984) Excitatory amino acids directly depolarize rat brain astrocytes in primary culture. Nature 311: 656-659.

Braun AR, Balkin TJ, Wesenten NJ, Carson RE, Varga M, Baldwin P, Selbie S, Belenky G, Herscovitch P (1997) Regional cerebral blood flow throughout the sleep-wake cycle. An H2(15)O PET study. Brain 120 (Pt 7): 1173-1197.

Brock LG, Coombs JS, Eccles JC (1952) The recording of potentials from motoneurones with an intracellular electrode. J Physiol 117: 431-460.

Brockhaus J, Deitmer JW (2000) Developmental downregulation of ATP-sensitive potassium conductance in astrocytes in situ. Glia 32: 205-213.

Carmignoto G, Pasti L, Pozzan T (1998) On the role of voltage-dependent calcium channels in calcium signaling of astrocytes in situ. J Neurosci 18: 4637-4645.

Casullo J, Krnjevic K (1987) Glial potentials in hippocampus. Can J Physiol Pharmacol 65: 847-855.

Celesia GG, Jasper HH (1966) Acetylcholine released from cerebral cortex in relation to state of activation. Neurology 16: 1053-1063.

Charara A, Smith Y, Parent A (1996) Glutamatergic inputs from the pedunculopontine nucleus to midbrain dopaminergic neurons in primates: Phaseolus vulgaris-leucoagglutinin anterograde labeling combined with postembedding glutamate and GABA immunohistochemistry. J Comp Neurol 364: 254-266.

Connors BW, Gutnick MJ, Prince DA (1982) Electrophysiological properties of neocortical neurons in vitro. J Neurophysiol 48: 1302-1320.

Consolo S, Bertorelli R, Forloni GL, Butcher LL (1990) Cholinergic neurons of the pontomesencephalic tegmentum release acetylcholine in the basal nuclear complex of freely moving rats. Neuroscience 37: 717-723.

Contreras D, Steriade M (1995) Cellular basis of EEG slow rhythms: a study of dynamic corticothalamic relationships. J Neurosci 15: 604-622.

Contreras D, Timofeev I, Steriade M (1996) Mechanisms of long-lasting hyperpolarizations underlying slow sleep oscillations in cat corticothalamic networks. J Physiol 494 (Pt 1): 251-264.

Corvalan V, Cole R, de Vellis J, Hagiwara S (1990) Neuronal modulation of calcium channel activity in cultured rat astrocytes. Proc Natl Acad Sci U S A 87: 4345-4348.

Darby M, Kuzmiski JB, Panenka W, Feighan D, MacVicar BA (2003) ATP released from astrocytes during swelling activates chloride channels. J Neurophysiol 89: 1870-1877.

Datta S, Siwek DF (1997) Excitation of the brain stem pedunculopontine tegmentum cholinergic cells induces wakefulness and REM sleep. J Neurophysiol 77: 2975-2988.

Duffy S, Fraser.D.D., MacVicar BA (1995) Potassium Channels. In: Neuroglia (Kettenmann H, Ransom BR, eds), pp 185-201. New York: Oxford Univ. Press.

Duffy S, MacVicar BA (1994) Potassium-dependent calcium influx in acutely isolated hippocampal astrocytes. Neuroscience 61: 51-61.

Elhusseiny A, Hamel E (2000) Muscarinic--but not nicotinic--acetylcholine receptors mediate a nitric oxide-dependent dilation in brain cortical arterioles: a possible role for the M5 receptor subtype. J Cereb Blood Flow Metab 20: 298-305.

Eng LF, Vanderhaeghen JJ, Bignami A, Gerstl B (1971) An acidic protein isolated from fibrous astrocytes. Brain Res 28: 351-354.

Franck G, Grisar T, Moonen G (1983) Glial and neuronal Na+, K+ pump. In: Advances in Neurobiology (Fedoroff S, Hertz L, eds), pp 139-159. New York: Academic Press.

Gardner-Medwin AR (1983) Analysis of potassium dynamics in mammalian brain tissue. J Physiol 335: 393-426.

Gardner-Medwin AR, Nicholson C (1983) Changes of extracellular potassium activity induced by electric current through brain tissue in the rat. J Physiol 335: 375-392.

Glenn LL, Steriade M (1982) Discharge rate and excitability of cortically projecting intralaminar thalamic neurons during waking and sleep states. J Neurosci 2: 1387-1404.

Godfraind JM, Kawamura H, Krnjevic K, Pumain R (1971) Actions of dinitrophenol and some other metabolic inhibitors on cortical neurones. J Physiol 215: 199-222.

Goldsmith M, van der Kooy D (1988) Separate non-cholinergic descending projections and cholinergic ascending projections from the nucleus tegmenti pedunculopontinus. Brain Res 445: 386-391.

Graeber MB, Streit WJ, Kreutzberg GW (1988) Axotomy of the rat facial nerve leads to increased CR3 complement receptor expression by activated microglial cells. J Neurosci Res 21: 18-24.

Grofova I, Zhou M (1998) Nigral innervation of cholinergic and glutamatergic cells in the rat mesopontine tegmentum: light and electron microscopic anterograde tracing and immunohistochemical studies. J Comp Neurol 395: 359-379.

Guthrie PB, Knappenberger J, Segal M, Bennett MV, Charles AC, Kater SB (1999) ATP released from astrocytes mediates glial calcium waves. J Neurosci 19: 520-528.

Hallanger AE, Wainer BH (1988) Ascending projections from the pedunculopontine tegmental nucleus and the adjacent mesopontine tegmentum in the rat. J Comp Neurol 274: 483-515.

Harris RJ, Symon L (1984) Extracellular pH, potassium, and calcium activities in progressive ischaemia of rat cortex. J Cereb Blood Flow Metab 4: 178-186.

Hosli E, Hosli L (1988) Autoradiographic localization of binding sites for muscarinic and nicotinic agonists and antagonists on cultured astrocytes. Exp Brain Res 71: 450-454.

Hosli E, Hosli L (1993) Receptors for neurotransmitters on astrocytes in the mammalian central nervous system. Prog Neurobiol 40: 477-506.

Hosli L, Hosli E, Della BG, Quadri L, Heuss L (1988) Action of acetylcholine, muscarine, nicotine and antagonists on the membrane potential of astrocytes in cultured rat brainstem and spinal cord. Neurosci Lett 92: 165-170.

Jones BE (1991) Paradoxical sleep and its chemical/structural substrates in the brain. Neuroscience 40: 637-656.

Jones BE, Cuello AC (1989) Afferents to the basal forebrain cholinergic cell area from pontomesencephalic--catecholamine, serotonin, and acetylcholine--neurons. Neuroscience 31: 37-61.

Kandel ER, Schwartz JH, Jessell TM (1991) Principles of neural science. McGraw Hill, 4th edition.

Kettenmann H, Schachner M (1985) Pharmacological properties of gamma-aminobutyric acid-, glutamate-, and aspartate-induced depolarizations in cultured astrocytes. J Neurosci 5: 3295-3301.

Krnjevic K, Pumain R, Renaud L (1971) The mechanism of excitation by acetylcholine in the cerebral cortex. J Physiol 215: 247-268.

Krnjevic K, Reinhardt W (1979) Choline excites cortical neurons. Science 206: 1321-1323.

Kuffler SW, Potter DD (1964) Glia in the leech central nervous system physiological properties and neuron-glia relationship. J Neurophysiol 27: 290-320.

Lavoie B, Parent A (1994) Pedunculopontine nucleus in the squirrel monkey: distribution of cholinergic and monoaminergic neurons in the mesopontine tegmentum with evidence for the presence of glutamate in cholinergic neurons. J Comp Neurol 344: 190-209.

Levi G, Gallo V (1995) Release of neuroactive amino acids from glia. In: Neuroglia (Kettenmann H, Ransom BR, eds), pp 815-826. New York: Oxford University Press.

MacVicar BA, Tse FW (1988) Norepinephrine and cyclic adenosine 3':5'-cyclic monophosphate enhance a nifedipine-sensitive calcium current in cultured rat astrocytes. Glia 1: 359-365.

MacVicar BA, Tse FW, Crichton SA, Kettenmann H (1989) GABA-activated Cl- channels in astrocytes of hippocampal slices. J Neurosci 9: 3577-3583.

Madsen PL, Vorstrup S (1991) Cerebral blood flow and metabolism during sleep. Cerebrovasc Brain Metab Rev 3: 281-296.

Maquet P (1997) Positron emission tomography studies of sleep and sleep disorders. J Neurol 244: S23-S28.

Massimini M, Amzica F (2001) Extracellular calcium fluctuations and intracellular potentials in the cortex during the slow sleep oscillation. J Neurophysiol 85: 1346-1350.

Meeker RB, Harden TK (1982) Muscarinic cholinergic receptor-mediated activation of phosphodiesterase. Mol Pharmacol 22: 310-319.

Metherate R, Cox CL, Ashe JH (1992) Cellular bases of neocortical activation: modulation of neural oscillations by the nucleus basalis and endogenous acetylcholine. J Neurosci 12: 4701-4711.

Metherate R, Tremblay N, Dykes RW (1988) The effects of acetylcholine on response properties of cat somatosensory cortical neurons. J Neurophysiol 59: 1231-1252.

Monyer H, Seeburg PH, Wisden W (1991) Glutamate-operated channels: developmentally early and mature forms arise by alternative splicing. Neuron 6: 799-810.

Moody WJ, Futamachi KJ, Prince DA (1974) Extracellular potassium activity during epileptogenesis. Exp Neurol 42: 248-263.

Moruzzi M, Magoun HW (1949) Brain stem reticular formation and activation of the EEG. Electroencephalogr Clin Neurophysiol 1: 455-473.

Murphy S, Pearce B (1987) Functional receptors for neurotransmitters on astroglial cells. Neuroscience 22: 381-394.

Newman EA (1986) High potassium conductance in astrocyte endfeet. Science 233: 453-454.

Newman EA (1995) Glial cell regulation of extracellular potassium. In: Neuroglia (Kettenmann H, Ransom BR, eds), pp 717-731. New York: Oxford Univ.Press.

Nicholson C (1995) Extracellular space as tha pathway for neuron-glia interaction. In: Neuroglia (Kettenmann H, Ransom BR, eds), pp 387-397. New York: Oxford Univ. Press.

Nunez A, Amzica F, Steriade M (1993) Electrophysiology of cat association cortical cells in vivo: intrinsic properties and synaptic responses. J Neurophysiol 70: 418-430.

O'Connor ER, Sontheimer H, Ransom BR (1994) Rat hippocampal astrocytes exhibit electrogenic sodium-bicarbonate co-transport. J Neurophysiol 72: 2580-2589.

Orkand RK (1986) Glial-interstitial fluid exchange. Ann N Y Acad Sci 481: 269-272.

Orkand RK, Nicholls JG, Kuffler SW (1966) Effect of nerve impulses on the membrane potential of glial cells in the central nervous system of amphibia. J Neurophysiol 29: 788-806.

Parpura V, Basarsky TA, Liu F, Jeftinija K, Jeftinija S, Haydon PG (1994) Glutamate-mediated astrocyte-neuron signalling. Nature 369: 744-747.

Pasti L, Volterra A, Pozzan T, Carmignoto G (1997) Intracellular calcium oscillations in astrocytes: a highly plastic, bidirectional form of communication between neurons and astrocytes in situ. J Neurosci 17: 7817-7830.

Pellerin L, Magistretti PJ (1994) Glutamate uptake into astrocytes stimulates aerobic glycolysis: a mechanism coupling neuronal activity to glucose utilization. Proc Natl Acad Sci U S A 91: 10625-10629.

Perea G, Araque A (2002) Communication between astrocytes and neurons: a complex language. J Physiol Paris 96: 199-207.

Perea G, Araque A (2003) [New information pathways in the nervous system: communication between astrocytes and neurones]. Rev Neurol 36: 137-144.

Porter JT, McCarthy KD (1997) Astrocytic neurotransmitter receptors in situ and in vivo. Prog Neurobiol 51: 439-455.

Privat A, Gimenez-Amaya M, Ridet JL (1995) Morphology of astrocytes. In: Neuroglia (Kettenmann H, Ransom BR, eds), pp 3-20. New York: Oxford University Press.

Quandt FN, MacVicar BA (1986) Calcium activated potassium channels in cultured astrocytes. Neuroscience 19: 29-41.

Ransom B (1995) Gap junctions. In: Neuroglia (Kettenmann H, Ransom B, eds), pp 299-318. New York: Oxford University Press.

Ransom CB, Sontheimer H, Janigro D (1996) Astrocytic inwardly rectifying potassium currents are dependent on external sodium ions. J Neurophysiol 76: 626-630.

Robert A, Magistretti PJ (1997) AMPA/kainate receptor activation blocks K+ currents via internal Na+ increase in mouse cultured stellate astrocytes. Glia 20: 38-50.

Rosier A, Arckens L, Orban GA, Vandesande F (1993) Immunocytochemical detection of astrocyte GABAA receptors in cat visual cortex. J Histochem Cytochem 41: 685-692.

Scarnati E, Gasbarri A, Campana E, Pacitti C (1987) The organization of nucleus tegmenti pedunculopontinus neurons projecting to basal ganglia and thalamus: a retrograde fluorescent double labeling study in the rat. Neurosci Lett 79: 11-16.

Semba K (1991) The cholinergic basal forebrain: a critical role in cortical arousal. In: The Basal Forebrain (Napier TC, Kalivas PW, Hanin I, eds), pp 197-218. New York: Plenum.

Semba K, Fibiger HC (1992) Afferent connections of the laterodorsal and the pedunculopontine tegmental nuclei in the rat: a retro- and antero-grade transport and immunohistochemical study. J Comp Neurol 323: 387-410.

Semba K, Reiner PB, Fibiger HC (1990) Single cholinergic mesopontine tegmental neurons project to both the pontine reticular formation and the thalamus in the rat. Neuroscience 38: 643-654.

Semba K, Reiner PB, McGeer EG, Fibiger HC (1988) Brainstem afferents to the magnocellular basal forebrain studied by axonal transport, immunohistochemistry, and electrophysiology in the rat. J Comp Neurol 267: 433-453.

Simon NR, Manshanden I, Lopes da Silva FH (2000) A MEG study of sleep. Brain Res 860: 64-76.

Singer W, Lux HD (1975) Extracellular potassium gradients and visual receptive fields in the cat striate cortex. Brain Res 96: 378-383.

Smiley KA, Lieberman EM (1980) Electrophysiological and pharmacological properties of glial cells associated with the medial giant axon of the crayfish with implications four neuron-glial cell interactions. Ups J Med Sci 85: 331-342.

Sofroniew MV, Priestley JV, Consolazione A, Eckenstein F, Cuello AC (1985) Cholinergic projections from the midbrain and pons to the thalamus in the rat, identified by combined retrograde tracing and choline acetyltransferase immunohistochemistry. Brain Res 329: 213-223.

Somjen GG (1979) Extracellular potassium in the mammalian central nervous system. Annu Rev Physiol 41: 159-177.

Sontheimer H, Kettenmann H, Backus KH, Schachner M (1988) Glutamate opens Na+/K+ channels in cultured astrocytes. Glia 1: 328-336.

Spann BM, Grofova I (1992) Cholinergic and non-cholinergic neurons in the rat pedunculopontine tegmental nucleus. Anat Embryol (Berl) 186: 215-227.

Steinhauser C, Gallo V (1996) News on glutamate receptors in glial cells. Trends Neurosci 19: 339-345.

Steininger TL, Wainer BH, Rye DB (1997) Ultrastructural study of cholinergic and noncholinergic neurons in the pars compacta of the rat pedunculopontine tegmental nucleus. J Comp Neurol 382: 285-301.

Steriade M, Amzica F (1996) Intracortical and corticothalamic coherency of fast spontaneous oscillations. Proc Natl Acad Sci U S A 93: 2533-2538.

Steriade M, Amzica F (1998) Coalescence of sleep rhythms and their chronology in corticothalamic networks. Sleep Res Online 1: 1-10.

Steriade M, Amzica F, Contreras D (1994a) Cortical and thalamic cellular correlates of electroencephalographic burst-suppression. Electroencephalogr Clin Neurophysiol 90: 1-16.

Steriade M, Amzica F, Contreras D (1996) Synchronization of fast (30-40 Hz) spontaneous cortical rhythms during brain activation. J Neurosci 16: 392-417.

Steriade M, Amzica F, Nunez A (1993a) Cholinergic and noradrenergic modulation of the slow (approximately 0.3 Hz) oscillation in neocortical cells. J Neurophysiol 70: 1385-1400.

Steriade M, Contreras D, Amzica F (1994b) Synchronized sleep oscillations and their paroxysmal developments. Trends Neurosci 17: 199-208.

Steriade M, McCarley RW (1990) Brain Control of Wakefulness and Sleep. New York: Plenum.

Steriade M, Nunez A, Amzica F (1993b) A novel slow (< 1 Hz) oscillation of neocortical neurons in vivo: depolarizing and hyperpolarizing components. J Neurosci 13: 3252-3265.

Steriade M, Nunez A, Amzica F (1993c) Intracellular analysis of relations between the slow (< 1 Hz) neocortical oscillation and other sleep rhythms of the electroencephalogram. J Neurosci 13: 3266-3283.

Steriade M, Oakson G, Ropert N (1982) Firing rates and patterns of midbrain reticular neurons during steady and transitional states of the sleep-waking cycle. Exp Brain Res 46: 37-51.

Steriade M, Timofeev I, Grenier F (2001) Natural waking and sleep states: a view from inside neocortical neurons. J Neurophysiol 85: 1969-1985.

Streit W (1995) Microglia cells. In: Neuroglia (Kettenmann H, Ransom BR, eds), pp 85-96. New York, Oxford University Press.

Sugimoto T, Hattori T (1984) Organization and efferent projections of nucleus tegmenti pedunculopontinus pars compacta with special reference to its cholinergic aspects. Neuroscience 11: 931-946.

Szerb JC (1967) Cortical acetylcholine release and electroencephalographic arousal. J Physiol 192: 329-343.

Takakusaki K, Shiroyama T, Yamamoto T, Kitai ST (1996) Cholinergic and noncholinergic tegmental pedunculopontine projection neurons in rats revealed by intracellular labeling. J Comp Neurol 371: 345-361.

Tanner LI, Harden TK, Wells JN, Martin MW (1986) Identification of the phosphodiesterase regulated by muscarinic cholinergic receptors of 1321N1 human astrocytoma cells. Mol Pharmacol 29: 455-460.

Tas PW, Massa PT, Koschel K (1986) Preliminary characterization of an Na+,K+,Cl- co-transport activity in cultured human astrocytes. Neurosci Lett 70: 369-373.

Teichberg VI (1991) Glial glutamate receptors: likely actors in brain signaling. FASEB J 5: 3086-3091.

Timofeev I, Steriade M (1996) Low-frequency rhythms in the thalamus of intact-cortex and decorticated cats. J Neurophysiol 76: 4152-4168.

Tong XK, Hamel E (2000) Basal forebrain nitric oxide synthase (NOS)-containing neurons project to microvessels and NOS neurons in the rat neocortex: cellular basis for cortical blood flow regulation. Eur J Neurosci 12: 2769-2780.

Trachtenberg MC, Pollen DA (1970) Neuroglia: biophysical properties and physiologic function. Science 167: 1248-1252.

Tse FW, Fraser DD, Duffy S, MacVicar BA (1992) Voltage-activated K+ currents in acutely isolated hippocampal astrocytes. J Neurosci 12: 1781-1788.

Ursin R (1968) The two stages of slow wave sleep in the cat and their relation to REM sleep. Brain Res 11: 347-356.

Van Der Zee EA, De Jong GI, Strosberg AD, Luiten PG (1993) Muscarinic acetylcholine receptor-expression in astrocytes in the cortex of young and aged rats. Glia 8: 42-50.

Van Der Zee EA, Matsuyama T, Strosberg AD, Traber J, Luiten PG (1989) Demonstration of muscarinic acetylcholine receptor-like immunoreactivity in the rat forebrain and upper brainstem. Histochemistry 92: 475-485.

Vazquez J, Baghdoyan HA (2003) Muscarinic and GABAA receptors modulate acetylcholine release in feline basal forebrain. Eur J Neurosci 17: 249-259.

Velasco A, Tabernero A, Granda B, Medina JM (2000) ATP-sensitive potassium channel regulates astrocytic gap junction permeability by a Ca2+-independent mechanism. J Neurochem 74: 1249-1256.

Villegas J (1975) Effects of cholinergic compounds on the axon-Schwann cell relationship in the squid nerve fiber. Fed Proc 34: 1370-1373.

Villegas R, Villegas L, Gimenez M, Villegas GM (1963) Schwann cell and axon electrical potential differences. Squid nerve structure and excitable membrane location. J Gen Physiol 46: 1047-1064.

Vincent SR, Satoh K, Armstrong DM, Fibiger HC (1983) Substance P in the ascending cholinergic reticular system. Nature 306: 688-691.

Wainer BH, Mesulam MM (1990) Ascending cholinergic pathways in rat brain. In: Brain Cholinergic Systems (Steriade M, Biesold D, eds), pp 65-119. Oxford: Oxford Univ. Press.

Walz W (1995) Acetylcholine ans serotonin receptor activation. In: Neuroglia (Kettenmann H, Ransom BR, eds), pp 346-353. New York: Oxford University Press.

Walz W, Hertz L (1982) Ouabain-sensitive and ouabain-resistant net uptake of potassium into astrocytes and neurons in primary cultures. J Neurochem 39: 70-77.

Winn P, Brown VJ, Inglis WL (1997) On the relationships between the striatum and the pedunculopontine tegmental nucleus. Crit Rev Neurobiol 11: 241-261.